HARVARD
School of Engineering
and Applied Sciences

Frank N. Keutsch
Stonington Professor of Engineering and Atmospheric Science
Professor of Chemistry and Chemical Biology
keutsch@seas.harvard.edu

Harvard John A. Paulson School of Engineering and Applied Sciences
Department of Chemistry and Chemical Biology
Department of Earth and Planetary Sciences
12 Oxford Street, Cambridge, MA 02138 USA
Phone: 617-495-1878 / Fax: 617-495-4902

November 10, 2020

Dear SCoPEx Advisory Committee,

In response to a written request by the Advisory Committee, we submit a document for a review of the scientific merits of SCoPEx.

In this document, we first review why existing observations are incapable of addressing questions that SCoPEx will answer. We then give a description of the basic design of the SCoPEx platform and its concept of operations. Finally, we describe the three science goals of SCoPEx, explain how they represent knowledge gaps for stratospheric aerosol injection (SAI), and specify what measurements are needed to enable SCoPEx to provide quantitative answers to these questions.

We do not provide a detailed engineering description of the SCoPEx platform nor of its scientific instrumentation. Nor do we provide a general justification for research on solar radiation modification. Finally, we do not provide a risk management plan, as that plan will be managed in coordination with the balloon operator and will depend on the specifics of the flight location and plan.

We look forward to working with the Committee and will be happy to revise these documents and provide additional materials on request.

Sincerely,

Frank Keutsch
Stonington Professor of Engineering and Atmospheric Science
Harvard John A. Paulson School of Engineering and Applied Sciences
Department of Chemistry and Chemical Biology
Department of Earth and Planetary Sciences

The Stratospheric Controlled Perturbation Experiment (SCoPEx)

Version 1.0

Executive Summary

Climate model studies of stratospheric solar radiation modification (SRM) depend, perhaps implicitly, on processes that take place in the near field of an injection plume. This is because materials delivered to the stratosphere by aircraft will form persistent, high aspect-ratio plumes with strong gradients before becoming well mixed, and processes within the plume will alter the large-scale, well-mixed aerosol and chemical properties that are simulated in global atmospheric models. All models ultimately depend on observations, yet we lack experimental data to assess some of the critical transport, microphysical, and chemical processes that directly control aerosol dynamics in the near-field that are important for understanding stratospheric SRM.

The scientific goal of the Stratospheric Controlled Perturbation Experiment (SCoPEx) is to improve process models that will, in turn, reduce uncertainties in global-scale models, thus reducing uncertainty in predictions of important SRM risks and benefits.

SCoPEx addresses questions in stratospheric aerosol injection (SAI) research that observations of existing analogues are incapable of addressing. For example, existing observational data do not include chemistry of alternate geoengineering materials specific to SAI, near-field particle microphysics of injection plumes, and relevant scales of atmospheric transport in the near-field. Yet these are needed to assess processes that control aerosol dynamics in the near field of an injection plume and that allow for the evaluation of alternate SAI materials, i.e., materials other than the naturally existing sulfate aerosol.

We first review why existing observations do not address the questions that SCoPEx will answer. We then give a description of the basic design of the platform and the concept of operations of SCoPEx. Finally, we describe the three specific science goals of SCoPEx, explain how they represent critical knowledge gaps in SAI research, and specify what measurements are needed to enable SCoPEx to provide quantitative answers to these questions. The three specific science goals are improving understanding of (i) turbulent mixing scales, (ii) aerosol microphysics with a focus on alternative SAI materials in the near-field of an injection, and (iii) process level chemical interactions of alternative SAI materials in the stratosphere.

We do not provide a detailed engineering document of the SCoPEx platform or its scientific instrumentation, nor do we provide a justification for the need for research on SRM via SAI in general. Rather, we focus specifically on the merits of SCoPEx itself.

1. Introduction

In this document we focus on the motivation and scientific merit of SCoPEx. We do not provide detailed engineering documentation of the SCoPEx platform or its scientific instrumentation. We also do not provide general justification for the need for research on solar radiation modification (SRM) via stratospheric aerosol injection (SAI), which can be found in many prior documents such as the 1992 NAS report that recommended the US government "Undertake research and development projects to improve our understanding of both the potential of geoengineering options to offset global warming and their possible side effects. This is not a recommendation that geoengineering options be undertaken at this time, but rather that we learn more about their likely advantages and disadvantages" (National Academy of Sciences et al., 1992) or the recent 2015 NAS report (National Research Council, 2015). Rather, we focus specifically on the need for small-scale field experiments such as SCoPEx, and the specific, critical SAI research needs that will be addressed by SCoPEx.

1.1. Role of and Need for Small-Scale Field Experiments

There is a vast array of science and engineering questions that have to be answered to achieve a better understanding of the risks, benefits and feasibility of SAI. The tools and topics that are needed to address these questions range from General Circulation Models (GCMs) all the way to detailed design of instrumentation to monitor or disperse aerosol. SCoPEx addresses a subset of questions that require small-scale field experiments for ground-truthing and that are aimed at improving the ability of models to predict the consequences of SAI.

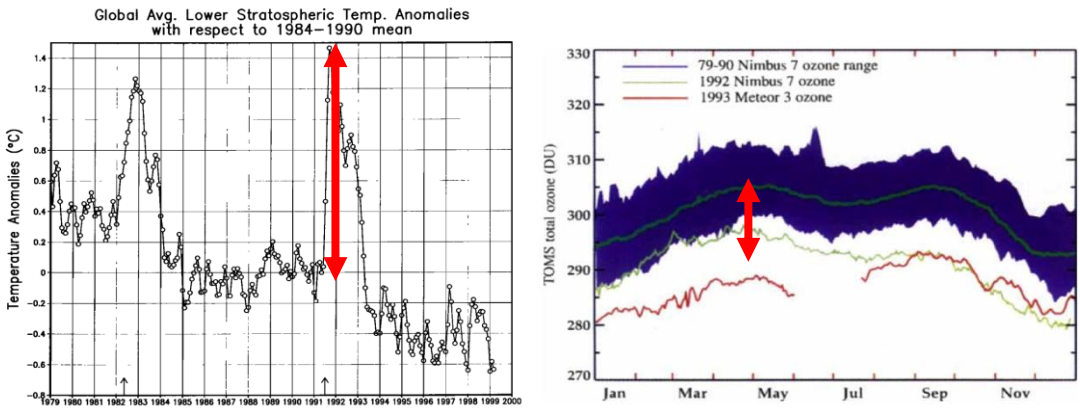

Figure 1: The two most important first-order stratospheric risks from sulfate SAI. The left panel shows stratospheric temperature anomalies from the El Chichon and Mount Pinatubo eruptions on top of background temperatures that are decreasing due to greenhouse gas emissions (Robock, 2000). The dynamical response of the stratosphere from such a short heating pulse likely is different than from sustained heating from longer-term SAI. The right panel shows that in the two years following the Mount Pinatubo reaction total ozone columns were lower than in the 1979-90 average as a result of increase sulfate aerosol surface area. Smaller eruptions also contributed to this. (McCormick et al., 1995)

There are numerous known risks associated with SAI, and SCoPEx focuses primarily on improving understanding of the first-order impacts in the stratosphere, i.e., risks and risk reduction associated with impacts of SAI within the stratosphere. There are many downstream / higher-order risks, e.g., impact on cloud formation as SAI particles leave the stratosphere (Cziczo et al., 2019), impacts on ecosystems via changes in the hydrological cycle (Bala et al., 2008; Russell et al., 2012; Tilmes et al., 2013), or the amount of direct

versus diffuse radiation (Gu et al., 2002; Farquhar & Roderick, 2003; Gu et al., 2003). Despite their importance, these impacts are not the direct target of this proposal although many of these are also influenced by stratospheric processes and properties of SAI aerosol. Two first-order risks are at the focus of this work: stratospheric ozone loss and the dynamic response resulting from stratospheric heating as a result of SAI.

Whereas stratospheric ozone chemistry is fairly well understood (World Meteorological Organization, 2019), there are still substantial uncertainties in the understanding and ability to model stratospheric dynamics (Figure 1). For example, models have only recently been able to reproduce the quasi-biennial oscillation without having it imposed (see Butchart et al., 2018 for a discussion of challenges). One approach taken in this work is to evaluate whether there are types of aerosols or methods of aerosol injection that can reduce first-order risks for a given amount of radiative forcing. It stands to reason that a reduction in the first-order stratospheric impacts will reduce downstream and higher-order risks. A case in point is the growing body of work that has been investigating the impacts of stratospheric heating on stratospheric water vapor and the dynamic response on regional climate (Simpson et al., 2019; Ferraro et al., 2015; Richter et al., 2018; Ji et al., 2018). It is important to note that the amount of stratospheric heating for a given material will be primarily driven by the total mass of aerosol, ozone destruction will be driven by the total surface area of aerosol, and the desired radiative forcing will be determined by the amount and size distribution of aerosol. Critically, both the aerosol mass required for a given desired radiative forcing *and* the resulting surface area are tied to this size distribution. Therefore, accurate models of the evolution of the size distribution of injected aerosol are critically needed. In addition, alternate materials with reduced stratospheric heating have to be investigated, as do injection methods for sulfate that minimize stratospheric heating and ozone loss for a given radiative forcing, as this will reduce risks associated with the dynamic response to this first-order perturbation.

2. Observational SAI Research Needs

Most of the rapidly growing body of literature on SAI rests on General Circulation Models (GCMs). We acknowledge the importance of GCM studies, but in the following we focus on research needs that require experiments and observations, and especially questions that can only be answered by conducting perturbative field experiments such as SCoPEx (see supplemental manuscripts Keith et al., 2020 and Floerchinger et al., 2020). In fact, SCoPEx will in the end inform GCMs by providing improved process level information that will be integrated in parameterizations used in GCMs. Below we review existing observational data sets and describe their utility for different SAI approaches, highlighting where they are unable to shed light on critical issues thus motivating studies like SCoPEx.

2.1. Field Experimental Needs for Sulfate SAI

Most studies that have sought to research SAI have assumed the addition of aerosol would take place by means of an injection of gas-phase SO_2, which is ultimately converted to H_2SO_4 and then to sulfate aerosol in the stratosphere on a timescale of approximately one month. The aerosol size distribution from this injection of gas phase precursor must be accurately predicted as it will control the shortwave (SW) scattering properties, the stratospheric lifetime of the aerosol, and ultimately be the driver for the radiative forcing (RF) efficiency per mass of injected sulfate. Some studies, such as Niemeier & Timmreck (2015), have suggested that with higher injection rates of SO_2, the resulting sulfate aerosol would be forced into a larger, coarse-mode size distribution and functionally reach a point of diminishing return. In this diminishing return scenario, the added amount of SW RF achieved per added mass of sulfate decreases exponentially.

Recent work by Pierce et al. (2010), Benduhn et al. (2016), and Vattioni et al. (2019) has highlighted the potential benefits of injecting H_2SO_4 aerosol directly into the accumulation mode (AM), i.e., aerosols with a radius of 0.1–1.0 μm, potentially by emitting H_2SO_4 vapor into an aircraft plume. This work has suggested better control of the resulting aerosol size distribution and thus the radiative forcing per unit mass sulfur injection, which would allow for the design of a system that maximizes the radiative forcing per mass of sulfate in a way that would not have the diminishing returns at high SO_2 injection rates. This would thus minimize the increase in the stratospheric sulfate burden and hence the risk of stratospheric heating which is driven by total mass whereas ozone loss is driven by surface area. While injecting AM–H_2SO_4 may represent the best possible approach for SAI with stratospheric sulfate, there is currently no proven way to introduce vapor phase AM–H_2SO_4 into the stratosphere. As AM–H_2SO_4 has not been studied, perturbative experiments are required to provide observational constraints on the aerosol size distributions predicted by models.

2.2. Field Experimental Needs for Alternate Aerosol Material SAI

Though sulfate aerosol does exist in the background stratosphere and there are some natural analogs of broad stratospheric sulfate injections (volcanic eruptions), it likely is not the optimal candidate for SAI. Alternative aerosol may be most appropriate in order to mitigate SAI risks (Teller et al., 1996; Crutzen, 2006; Ferraro et al., 2011; Ferraro et al., 2015; Weisenstein et al., 2015; Keith et al., 2016; Dykema et al., 2016; Weisenstein et al., 2015). These alternate aerosols could reduce the previously noted two major first-order stratospheric impacts, i.e., changes in ozone and stratospheric heating. Due to the uncertainties in the impacts of stratospheric heating, the study of materials with optical

properties that negate stratospheric heating is especially important. Materials such as calcium carbonate ($CaCO_3$), alumina (Al_2O_3), diamond (carbon), and several others, have been proposed as a way to minimize the inherent risks from SAI (Keith et al., 2016; Dykema et al., 2016; Weisenstein et al., 2015; Ferraro et al., 2015; Ferraro et al., 2011; Crutzen, 2006). Although model results of these aerosol species suggest that some of them possess optical properties that make them well suited to be used in a SRM scenario ($CaCO_3$, Al_2O_3, and diamond) (Dykema et al., 2016; Ferraro et al., 2011), the stratospheric aerosol microphysics of these compounds (especially coagulation) is poorly understood. As with AM–H_2SO_4 injections, there is a profound lack of in situ data to assess the ability to model the microphysics of alternative aerosols and the stratospheric chemistry of these materials. This is especially pertinent with respect to changes in ozone, and is exacerbated by the fact that these aerosols have no naturally existing analog in the stratosphere that could be studied. Because early studies suggest that these aerosols show much promise with respect to deploying SAI while mitigating the inherent risks of the deployment, it is imperative to design and execute in situ experiments in order to test our current understanding of the aerosol microphysics and observe the effects of alternative aerosol on the chemical composition and dynamics of the stratosphere.

2.3. Limitations in Existing Analogues

In this section we will review previous in situ studies of stratospheric plume processes, show how those datasets have contributed to our current understanding, and demonstrate the need for experiments such as SCoPEx to inform small-scale models of aerosol microphysics (nucleation and coagulation), plume transport and physical morphology, and chemical properties of new aerosol species that have thus far not been observed in the stratosphere. Because the nature of the injection scenarios (AM–H_2SO_4 or solid aerosols) are so complex compared to natural analogs, new experiments must be designed and implemented to provide observational constraints on our current nearfield modeling framework. Experimental data from carefully targeted small-scale studies would contribute to the development of nearfield-scale models that represent currently uncertain processes in detail.

We note that sub-grid scale processes do not represent the only unknowns in GCMs that are relevant to high-fidelity simulations of SRM scenarios, and that there are many large scale model phenomena which should be further assessed with observational evidence. However, here we focus on the need for in situ data to constrain sub-grid scale processes that can be addressed by SCoPEx and highlight the need for reducing the uncertainty in transport and aerosol dynamics and chemistry at this scale.

2.3.1. Limitations of Solid Rocket Motor Plume Observations

From 1996 to 2000 a number of rocket plumes were observed by high-altitude research aircraft. Generally, these missions involved a research team coordinating stratospheric sampling flights on either the NASA ER-2 or on the NASA WB-57 with coincident rocket launch events from either Cape Canaveral or Vandenberg Airforce Base. These studies sampled plumes from a host of rocket types including Titan IV, Space Shuttle (STS106, STS83, STS85), Delta II, Athena II, and Atlas IIAS.

Plumes were intercepted by the sampling aircraft between 5 and 125 minutes after emission from the rocket motor at stratospheric altitudes ranging from 11 to 19.8km (Voigt et al., 2013). The main science objective of these missions was to assess the stratospheric

ozone depletion potential of space exploration by understanding the halogen chemistry occurring as a result of the high-altitude rocket burn. However, in studying the effects on the ozone layer, this era of stratospheric sampling provided a unique set of plume measurements to study nearfield processes of chemical injections into the stratosphere.

While measuring the plumes from the Titan IV rocket (as a part of the United States Airforce Rocket Impacts on Stratospheric Ozone (RISO) Campaign) and attempting to develop a plume chemistry model to solve for the Cl_2 concentration in a rocket plume as it evolves shortly after its emission, Ross et al. (1997) noted the many assumptions that had to be made about the plume morphology in order to simulate the mixing and diffusion that the rocket plume had with the surrounding stratosphere. Their model solved for the Cl_2 concentration of a circular nighttime plume as it expanded in diameter along an isentropic surface. Subsequent aircraft measurements showed that plumes contained more than twice the predicted concentration of Cl_2 despite the plume being intercepted during the day time (when the Cl_2 reservoir should be somewhat depleted by the photolysis reaction $Cl_2 + h\nu \rightarrow 2Cl$), suggesting that there may be an error in the assumption of a circular plume morphology on the short transport time scales observed in this study ($\sim 28 min$).

Ross went on to publish a second study as a part of the RISO project in 1999, this time looking to quantify the size distribution of alumina aerosols emitted from the rocket engines which contained particulate alumina (Al_2O_3) (Ross et al.,1999). They compared measured aerosol size distributions from the WB-57F plume interceptions to results from an aerosol coagulation model and highlighted a massive discrepancy. The model predicted a much smaller aerosol size distribution with 1-10% of the aerosol mass being in the smallest (0.005µm) mode and the aircraft observed only fractions (<0.05%) of the model estimate in that same small mode. At the same time, over 99% of the aerosol mass sampled by the aircraft was found in the coarsest mode (2 µm), which the model was unable to predict. It is most likely that the model used in Ross et al. (1999) did not well account for the effects of ion mediated nucleation as described by Yu & Turco (1997). However, the data from Ross et al. (1999) was some of the first in situ data to highlight the uncertainty in stratospheric aerosol coagulation models. Alumina aerosol, as well as other solid aerosols, in contrast to liquid sulfate aerosol, have since been investigated as a candidate for use in SAI (Weisenstein et al., 2015). Therefore, it is imperative that we understand the chemical, coagulation, and accumulation properties of these and other solid aerosols in a stratospheric environment.

2.3.2. Limitations of Previous Stratospheric Aircraft Wake Crossing Observations

We can look to the few times high-altitude aircraft wake plumes have been sampled in situ for another example of stratospheric plume measurements. In the early 1990s the popularity and capability of the Concorde spurred discussions of a large fleet of High Speed Civil Transport (HSCT) aircraft that would operate in the lower stratosphere between 16 and 23 km. Scientists became concerned with the effects of high-altitude aircraft and high-altitude supersonic aircraft on stratospheric ozone destruction via the creation of a large NOx source in the lower stratosphere. NASA then launched several field campaigns using the ER-2 to study the exhaust profiles of high-altitude aircraft. In 1992 NASA commissioned the Stratospheric Photochemistry Aerosols and Dynamics Expedition (SPADE) to look at the effects of HSCTs. As a part of SPADE the ER2 sampled its own plume on several occasions by making a hairpin turn and heading into its original path, therefore measuring its own wake

(Figure 2). SPADE resulted in at least 11 published studies and some of these can inform us about the mixing and aerosol dynamics that may be relevant to an SAI scenario (Stolarski & Wesoky, 1993).

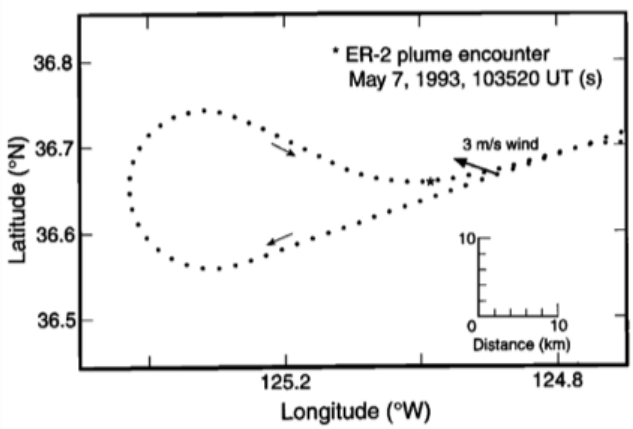

Figure 2: Shows the ER-2 flight track on a typical wake crossing trajectory (adapted from Fahey et al. 1995).

Fahey et al. (1995a) described measurements made of condensation nuclei (CN) present in the ER-2's exhaust plume from the emission of aerosol carbon and of sulfur compounds during one of its SPADE wake crossing events. Because the main focus of this study was to quantify the emission indices (EIs) of various compounds measured by the ER-2 that may have ozone depletion implications, they focused mainly on gas phase compounds. However, for the three wake crossings that the study focused on, they observed large variability in their EI measurements for CN. They noted that this is likely due to differences in mixing history of the encountered air parcels and noted that a full explanation of CN coagulation required more in-depth study and further measurements (Fahey et al, 1995b).

In another study published by Fahey et al. (1995b), they used a similar wake crossing technique to measure the exhaust of the Concorde aircraft and developed an aerosol coagulation model to predict particle formation and size as a function of the time since emission from the aircraft. The coagulation model was initialized at the observed conditions from the one-hour old Concord transect. The results from this model estimated that from 0 to 10 hr since emission from the engine, the mean particle diameter remained fairly constant at 0.06 μm before growing exponentially to a factor of 3 times its initial value over the next 1,000hr. The model predicted exponential mean particle diameter growth continuing right until the of the simulation at 1,000 hr (Fahey et al., 1995a).

Yu & Turco (1997) attempted to model the observed aerosol plume during the Concorde wake crossings with the goal of determining the driving factor for the large aerosol size distributions observed by the ER-2 in the exhaust which had not yet been explained by models. Yu proposed that aerosol formation was being aided by ion-mediated nucleation (IMN), that is, charged particles formed by chemi-ionization processes within the aircraft engines provide charged centers (H_2SO_4 [S(VI)]) around which molecular clusters rapidly coalesce. "The resulting charged micro-particles exhibit enhanced growth due to condensation and coagulation aided by electrostatic effects" (Yu & Turco, 1997). It is likely that IMN is the reason previous particle coagulation modeling of solid rocket motor plumes had overestimated the amount of aerosol in the small size ranges when compared to the in situ data, though this has not since been tested. Because of these effects, and the fact that specific size distributions of aerosol are desired to obtain the optimal radiative

forcing effects for SAI (nominally smaller than observed in rocket or aircraft plumes), we must understand the aerosol nucleation and coagulation dynamics in an unperturbed stratosphere.

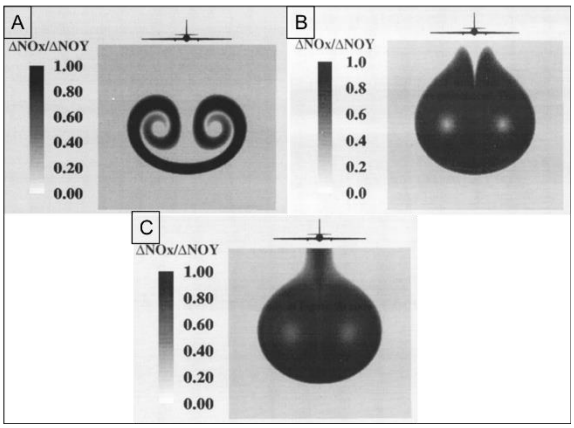

Figure 3: Shows the chemical and morphological evolution of an ER-2 plume during SPADE at 1.7 km (A), 4.8 km (B), and 7.9 km (C). (adapted from Anderson et al. (1996))

As a part of the SPADE project, Anderson et al. (1996) computed the flow field and chemical kinetics of the ER-2 aircraft exhaust using the Aerodyne Research Inc. UNIWAKE model. Their calculations address the effects of complex plume morphology on in-plume chemistry as a function of dilution time since emission from the aircraft engine. They showed that the plume morphology is highly variable out to about 5 km post emission Figure 3 and estimated that the stability of the wing vortex pair begins to break up at roughly 20 km post emission. Although this study was completed in the mid 1990s, it is still one of the only studies that attempts to compute nearfield chemistry within a dynamic stratospheric plume. However, particles were not considered as part of this study.

2.3.3. Limitations of Stratospheric Wake Crossings

Previous stratospheric plume studies of solid rocket motors and aircraft wake crossings have laid the foundation for our understanding of stratospheric plume chemical, aerosol, and mixing dynamics on transport scales of 0→100 km. These studies highlight the types of processes we must be aware of when considering the logistics of SAI. However, the violent initial conditions of engine exhaust plumes (such as temperatures of 700K, IMN) make it difficult to relate these observations to other systems. Because the engines drive the mixing and transport in the nearfield, and the ionic injection conditions of the plume create electrostatic forces that introduce complex nucleation affinities (IMN), understanding individual parameters can become analogous to finding a needle in a haystack. Moreover, because the radiative properties of any stratospheric aerosol that may be used for SRM depend on the diameter of the particle, we must understand the coagulation of that aerosol in the nearfield after the injection, which means that we must also understand the plume morphology that dictates the concentrations of that aerosol. Currently there have been no in situ data gathered that help us understand nearfield aerosol nucleation and plume dynamics in the absence of a very disruptive source. These conditions are necessary to understand as SAI may require that we mitigate the effect of IMN in order to obtain an aerosol size distribution that is small enough to provide the desired radiative properties.

2.3.4. Limitations of Naturally Occurring Analogs

Another source of useful in situ data on plume dynamics in the stratosphere can be found in literature addressing the fate and transport of convective overshooting events that often occur at the top of a Mesoscale Convective Complex (MCC). These events drive brief airmass exchange with the troposphere and often end up resulting in a plume-like parcel of tropospheric air being injected into the stratosphere.

Measurements of convective systems and upper troposphere-lower stratosphere exchange, as a means to interrogate stratospheric plume transport, have provided valuable in situ datasets that help us understand mid-field (10 to >1000 km) plume dynamics in the lower stratosphere. Similar to convective overshooting events, volcanic eruptions have provided an immense amount of in situ data that has informed us about regional and even global transport of stratospheric injections (Robock, 2000). Although their data are applicable in some sense to the transport of an SAI plume after its initial injection, the turbulent nature of a convective storm makes it difficult to measure these events at points near their injection source. Additionally, the storm conditions themselves dramatically complicate the system in the lower stratosphere such that is difficult to see through the effects of the induced turbulence in the nearfield. Indeed, an important limitation of these type of natural analogs is the spatial extent of their perturbation, which does not allow for near-field observations analogous to that of a point source. This also arises from the violent nature of these events which does not allow airborne platforms, such as the ER-2, to sample the initial conditions of the injection. We also note that volcanic eruptions are limited in their utility to evaluate dynamic response to stratospheric heating from sulfate aerosol, as they represent a perturbative pulse rather than the long-term heating one would expect from SAI.

In addition, these natural analogues provide extremely limited ability to study alternate materials, although organic and mineral dust aerosol injections into the lowermost stratosphere have been documented from convective overshoots. However, the complexity of the massive perturbations of both gas- and particle-phase preclude a study focusing on the impact on stratospheric composition and aerosol evolution that would result from SAI of a single material.

3. SCoPEx Short Overview

This section provides a brief overview of the engineering and operational aspects of SCoPEx. We first describe the platform, the instruments, and the concept of operations before describing the rationale for the overall SCoPEx design choices.

3.1. SCoPEx Platform

The SCoPEx gondola (Figure 4) is a balloon-born new research platform being developed at Harvard by the engineering and science staff within the Anderson/Keith/Keutsch laboratory group. The development builds on four decades of stratospheric research on aircraft, balloon, and rocket platforms that has focused on understanding the environmental chemistry of the ozone layer. The SCoPEx experiment was first described by Dykema et al. (2014). While many details of the design have changed, that paper still succinctly describes the advantages of choosing a balloon born platform over an aircraft, particularly for studying perturbations like solar geoengineering, and several of the limits of laboratory experiments that that could be addressed in a perturbative experiment like SCoPEx.

The gondola has three primary features: the frame, the ascender, and the propellers. The aluminum and carbon fiber frame contains two decks and a ballast hopper for coarse altitude control. One deck is primarily dedicated to platform support (power and flight control) and one deck is primarily dedicated to instruments. At the top of the gondola is an ascender and rope which allows the distance between the bottom of the balloon train and the gondola to vary from 0 to 150 m, which provides fine altitude control of the gondola. The ascender has been developed and tested by Atlas (Chelmsford, MA) building on their previous hardware in collaboration with the Harvard engineering team. The propellers serve two purposes: to create a well-mixed volume of air where observations of the aerosols and perturbed gas-phase can be made, and to reposition the gondola within the evolving aerosol plume. While the trajectory of the balloon and gondola system will be dictated by the balloon, the propellers allow for repositioning relative to the prevailing winds.

The ascender makes it impossible to have cables and other physical connections between the flight operations equipment and the gondola. Thus, the platform will handle its own communications and power. The SCoPEx platform will be powered using 28 V and 100 V DC power supplies which will power all operations on the platform including the propellers, ascender, and instruments. Elements of the flight platform are listed in Table 1. The gondola flight, flight safety, recovery parachute, and recovery operations will be managed by the balloon operator (in contrast to the SCoPEx team itself). Because the absolute velocity and distance capability of the gondola are so small compared to balloon drift, the trajectory will be determined by the balloon operator as if it was a passive nonpowered payload. During operations, the detailed float altitude will be jointly managed by the balloon operator via control of the balloon vents and the Harvard team via control of the ballast and ascender.

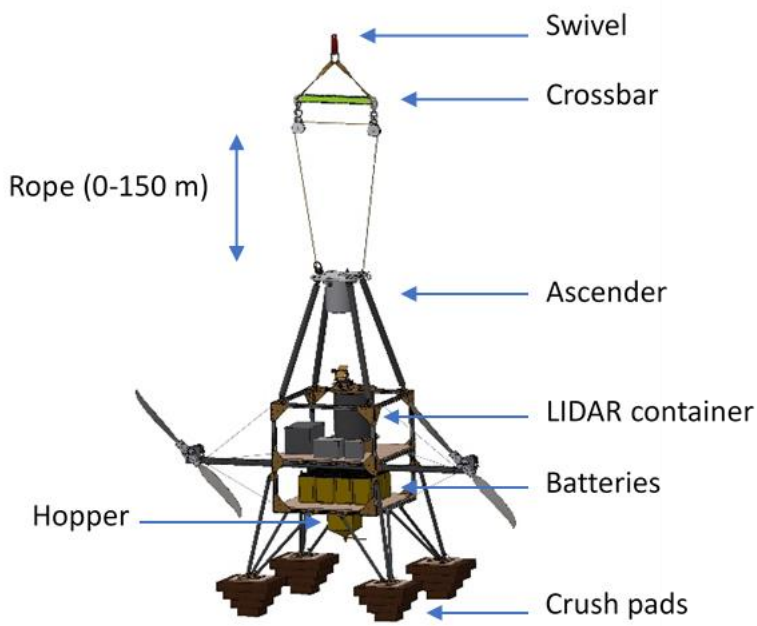

Figure 4: A representation of the SCoPEx flight platform. The final configuration may have subsystems packaged differently.

Parameter	**Description**
Total mass (Frame, all subsystems, hopper with ballast)	600 kg
Interface to balloon	Crosby 5-S-2 jaw & jaw swivel
Ascender	13 mm diameter rope Range of motion: 0-150 m Max speed: 10 m/min
Gondola propulsion	Twin propellers, 1.88 m diameter 32 N thrust each Max airspeed: 3 m/s
Power	28 V and 100 V DC power supplies with 24 MJ and 10 MJ total energy when fully charged
Communications	Satellite phone for communication between ground equipment and payload
Maximum termination shock	10 g

Table 1: Elements of the SCoPEx flight platform.

3.2. Instruments for First Science Flights (Science Goals 1 and 2)

The proposed instruments for the first science flight, addressing science Goals 1 and 2, are listed in Table 2. The corresponding science goals that motivate their inclusion are detailed in Section 4.

Measurement	Instruments	Rationale	Corresponding Science Goal
Wind speed measurement	Wind pendulum	Gondola and plume movement relative to balloon	Platform operation
Meteorology	Commercial off-the-shelf instrument	Temperature and pressure measurement throughout the flight	1, 2, 3
Wind turbulence	Constant temperature anemometer	Stratospheric mixing and modeling evolution of aerosol size distribution	1, 2
Particle dispersal	Solid Aerosolizer	Injects monodispersed particles for measurement and study	2, 3
Plume tracking	LIDAR	Tracking plume and navigation back into plume	2, 3
Particle sizer	POPS	Aerosol size distribution measurement for comparison with microphysics models of near-field evolution	2, 3
Light Scattering	Radiometer	Comparison of aerosol scattering with model prediction	2

Table 2: Instruments for first SCoPEx science flight.

Wind Pendulum: Understanding differential wind speed measurements between the balloon and payload will be important for plume evolution relative to the balloon trajectory and navigating the payload back into the plume. Commercial equipment to measure wind speed is typically not designed for the low densities found in the stratosphere. SCoPEx will therefore use a pendulum-based instrument and model to extract wind speed measurements. A camera will track a pendulum bob with high surface area and low mass, light enough to be perturbed by low winds in the stratosphere. Using the location and tilt data from the payload and a 3-dimentail kinetic model, the wind speed will be extracted from photos of the pendulum bob.

Commercial Meteorology Instrument: Commercial off-the-shelf instruments will be used for meteorological measurements on SCoPEx. They will record pressures and temperatures of the ambient stratosphere.

Constant Temperature Anemometer: A constant temperature anemometer (CTA) uses convective cooling caused by air flowing across a heated thin wire to measure flow velocity. LITOS (Leibniz-Institute Turbulence Observations in the Stratosphere) (Gerding et al., 2009; Theuerkauf et al., 2010) used such a measurement to study stratospheric turbulence up to 29 km. LITOS consisted of a 5 μm diameter and 1.25 mm long tungsten wire CTA and a 16 bit ADC with 2000 samples per second to collect measurements with a vertical resolution of 2.5 mm at 5 m/s ascent speed. The anemometer data was analyzed by performing a spectral

analysis on the voltage signal to retrieve the spectral slope of the observed variation. A similar instrument will be used on SCoPEx to measure stratospheric turbulence. Air flow around the device will be simulated using CFD tools. The CFD runs will provide a means to identify key flow characteristics that drive sensor performance (sensitivity and accuracy), and to drive detailed sensor design.

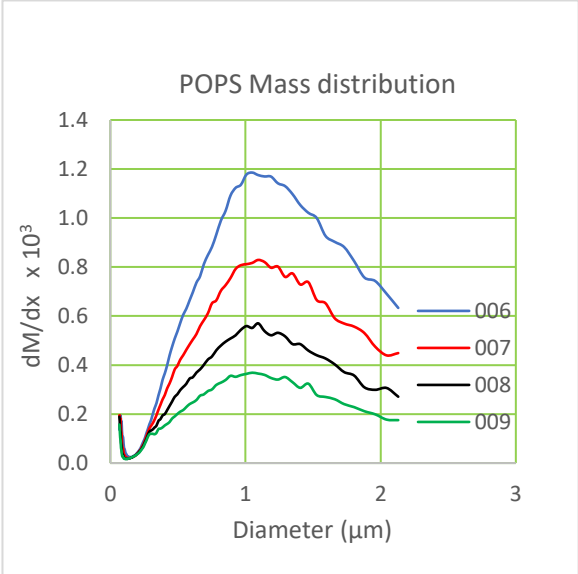

Figure 5: Successive measurements of sprayed $CaCO_3$ using an optical particle spectrometer. 006-009 indicate numbered time intervals spaced 4 minutes apart with 006 being the earliest measurement. $CaCO_3$ was sprayed using a 200 µm nozzle. In this laboratory experiment there was no significant variation in the shape of the distribution over time. (personal communication A Neukermans and team)

Solid Aerosolizer: The solid particle aerosolizer has been developed by a team lead by Armand Neukermans. For SCoPEx, the goal is to spray roughly monodisperse ~0.5 µm diameter precipitated calcium carbonate powder, the first candidate for solid SAI, through a 1-2 mm nozzle using the expansion of powder suspended in high pressure liquid CO_2. The aerosolizer would use a 1:4 weight ratio of $CaCO_3$ to CO_2. For 1 kg of $CaCO_3$ this would require a 5-7 L pressurized container. This concept has already been demonstrated in the lab. Figure 5 shows successive measurements of sprayed $CaCO_3$ with a size distribution centered at 1 µm diameter. Measurements were taken every 4 minutes using POPS (see below). In this case, total particle count decreased over time but there was no significant variation in the shape of the size distribution.

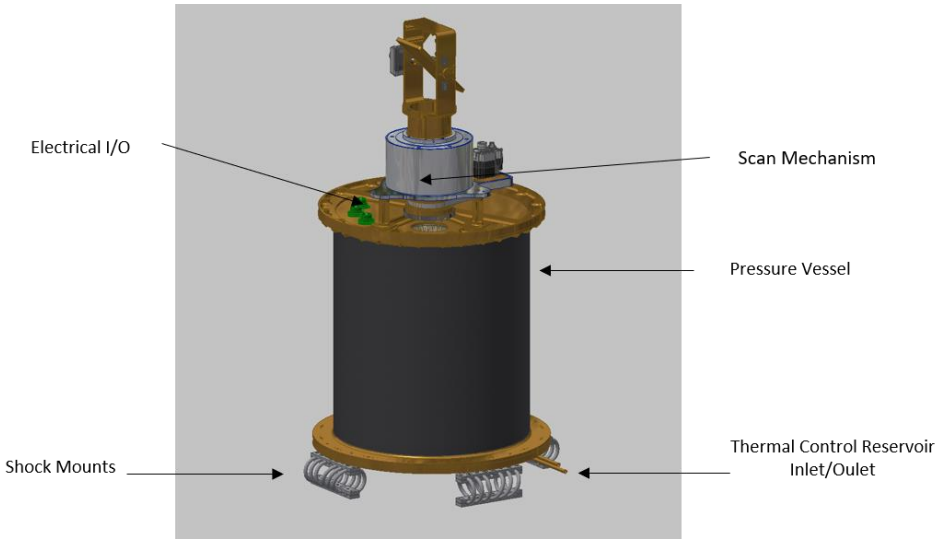

Figure 6: LIDAR pressure vessel provides safe storage and operating environment and support equipment.

LIDAR: The LIDAR is used to track the plume and allow navigation back into it. The core of the LIDAR system is an off-the-shelf eye-safe visible LIDAR, purchased from Sigma Space (now owned and operated by Droplet Measurement Technologies). This LIDAR produces 4 µJ pulses of 532 nm light at a repetition rate of 532 nm. The light that is backscattered by molecules and aerosols is collected by an 80 mm telescope and detected with a high-speed, high-sensitivity photodiode.

We have integrated this LIDAR in a pressure vessel (Figure 6) to provide a near-1 atm pressure environment with adequate temperature stability to ensure safe operation of the LIDAR at float altitude and safe storage on launch, ascent, descent, and recovery. This pressure vessel includes equipment for electrical and mechanical support, including command, data handling, and shock mounting. The LIDAR requires a scan capability to search the nearby atmosphere for the extent and geometry of the plume. The tilt and pan functions of the scan capability allows the LIDAR to be scanned over a set of angles that define the plausible location of the plume.

Portable Optical Particle Spectrometer (POPS): The POPS instrument will provide the aerosol size distribution measurements for studying aerosol formation and agglomeration. POPS is a light-weight instrument that directly samples the aerosol. It was built by and provided to SCoPEx through a collaboration with NOAA. The particles are illuminated with a 405 nm diode laser and the scattered light is collected onto a photomultiplier tube. The particle size is determined by the intensity of the scattered light. It has both the detection limit and size range (0.13 – 3 µm) to measure background stratospheric aerosol, which is more than sufficient for SCoPEx needs (Gao et al., 2016).

The Keutsch Group has already developed and extensively characterized a POPS instrument in preparation for the NASA-EVS3 Dynamics and Chemistry of the Summer Stratosphere field campaign on board the NASA-ER2, for which Keutsch is the deputy-PI. The POPS instrument tests include extensive thermal vacuum chamber characterizations to ensure operation under harsh stratospheric conditions. Compared to the ER-2, operation for SCoPEx will be simpler due to the insignificant air speed of the balloon and a much simpler operational pressure regime (on the ER-2 there is a large range of external pressures for both sampling and exhaust).

Radiometer: The aerosol plume can also be detected using a narrowband, narrow field of view radiometer with azimuthal/zenith pointing capability. The relationship between measurements of scattered solar radiation and the physical characteristics of atmospheric aerosols has been studied for more than two decades. Sky scanning measurements at multiple wavelengths between 300 nm and 1200 nm have been obtained using robotically pointed ground-based spectral radiometers deployed worldwide (Holben et al., 1998). The theory of these measurements has been refined and validated as a function of viewing geometry to provide a strong basis for inferring aerosol microphysics from radiometer data (Torres et al., 2014). The success of these approaches has motivated the development of compact sky scanning radiometers suitable for deployment on unsteady platforms like unmanned aerial vehicles (UAVs) and SCoPEx. One such design, reported by NOAA (Murphy et al., 2016), measures at 4 wavelengths (460 nm, 550 nm , 670 nm, and 860 nm) with a field of view of 0.006 sr (equivalent to 2.5° half-angle) and a circular limiting aperture of 1.1 mm diameter. A radiometer like this one deployed on SCoPEx would be capable of observing a SCoPEx plume, based on Golja et al. (2020), formed by a 0.1 g s^{-1} injection of calcite from a distance of 200 m with an approximate signal-to-noise ratio of 6000 for a 1 ms signal accumulation.

3.3. Instruments for Future Science Flights (Science Goal 3)

The additional instruments listed in Table 3 are candidates for future SCoPEx flights beyond the initial science flight, i.e., addressing science goal 3. They have not yet been adapted to fly on the SCoPEx platform. Instrument choices will be refined based on experiences in the first science flights. The corresponding science goals that motivate their inclusion are detailed in Section 4.

Measurement	Candidate Instrument	Rationale	Corresponding science goal
Aerosol composition	Drum Sampler	Collecting aerosols for offline analysis	3
Water Vapor	IR Absorption or Frost Point	H_2O outgassing of platform, Influence on coagulation and heterogenous chemistry	2, 3
Atmospheric trace gas concentrations (ex: HCl, NOx)	Spectroscopic trace gas instruments	For measuring concentrations of various atmospheric trace gases before and after addition of solid ASI material	3

Table 3: Potential instrument for future SCoPEx science flights.

Aerosol Composition: Aerosol composition can be analyzed via the collection of aerosol with a drum sampler followed by offline analysis in the laboratory using standard offline methods. Aerosol sampling has been done numerous times aboard stratospheric platforms.

Water Vapor: Gas-phase water vapor measurements are important as relative humidity likely has a large impact on the heterogeneous reactivity of solid SAI material. The balloon and gondola can outgas significant amounts of water and thus an initial experiment will characterize how long, if at all, this outgassing perturbs the SCoPEx plume. As mentioned previously, the goal of SCoPEx is to ideally minimize the perturbation to only the introduction of calcium carbonate. Water vapor measurements are common on many stratospheric platforms.

Hydrogen Chloride: HCl can be measured via infrared absorption spectroscopy. The Anderson group at Harvard, which shares a laboratory with the Keutsch group, has developed a stratospheric HCl instrument and thus has extensive experience with the design of stratospheric HCl instrumentation. In addition, the Keutsch group has designed multiple spectroscopic trace gas measurements. The much lower air speeds of the balloon compared to aircraft favor the design of an open path system, which eliminates the notorious wall effects that can make HCl measurements challenging.

NOx: For NOx there exist a number of good instrumentation options. Recently, a compact NO-LIF instrument has been designed that has spectacular detection limits in the low ppt range, more than sufficient for the needs of SCoPEx. The instrument is a close analogue of the fiber-laser based formaldehyde LIF instrument that the Keutsch Group developed, so there is a high degree of expertise available for such an instrument. There are also sensitive cavity enhanced techniques available usually in the visible range of the spectrum.

3.4. SCoPEx Concept of Operations

Flights will proceed in the following manner. The payload would be launched with the ascender retracted such that there is minimal distance between the crossbar and platform. Once the balloon reaches the float altitude, the rope will be let out through the ascender such that there is 100 m between the crossbar and platform. The platform will then be ready to perform experiments and execute maneuvers. Figure 7 illustrates a proposed flight maneuver. The platform will initially travel in a straight line laying out a plume, after which it will maneuver back through the plume to make measurements. During these maneuvers the ascender can be used to fine tune the altitude of the platform and instruments. Several series of such maneuvers can be performed within each flight. At the conclusion of the experiments the ascender retracts the rope before the descent.

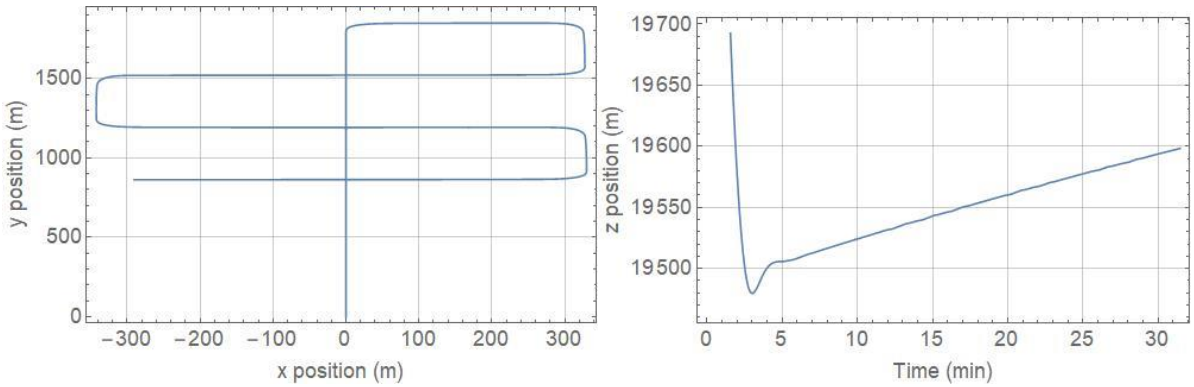

Figure 7: (left) A top down view of the proposed flight maneuvers over a 35-minute window. x and y are in the horizontal plane. The platform begins at (0,0). (right) The vertical position expected without any ascender or hopper vertical trimming over the same 35-minute platform maneuver.

4. SCoPEx Goals

In this section we describe the three long-term SCoPEx science goals. For each goal we describe the scientific problem, the need for SCoPEx, and the measurements required. The first phase of science flights targets the first two science goals. The design of the flights for the third goal will be informed by an understanding of the evolution of particle size distribution in the plume and the plume size. Thus, if later stage science flights move forward, they will be refined based on the results of the first science flights and the most up-to-date knowledge within the solar geoengineering and stratospheric science research communities.

4.1. Goal 1: Measurements of Turbulence for Small-Scale Mixing

4.1.1. The Importance of Plume-Scale Turbulence

Stratospheric turbulence influences the evolution of aerosol distribution from plume to regional to global scale. The mixing of air masses (of differing composition) in the stratosphere is a combination of two processes (Nakamura, 1996; Schoeberl & Bacmeister, 1993). The first process is strain, the distortion of streamline flow that brings air masses of differing composition adjacent to one another (Prather& Jaffe, 1990). Sometimes this is also referred to as “stirring” (Haynes, 2005). The second process occurs when air masses of differing composition are transported across the streamlines. This second process is the true “mixing” process.

In the stratosphere, mixing ultimately occurs because of molecular diffusion. This happens at the length scale of molecular viscosity. It is accelerated by turbulence, which can dramatically enhance the rate at which differing air masses are deformed to small enough spatial scales for molecular diffusion to mix them efficiently. Stratospheric turbulence is, however, highly intermittent (Vanneste, 2004). Understanding the mechanisms of stratospheric turbulence production is essential to understanding the spatial inhomogeneity and effective rate of mixing on spatial scales of 10-500 m (Schneider et al., 2017).

An understanding of this role of turbulence is of interest to stratospheric science because studies suggest that more accurate representations of mixing influence tracer distributions (Hoppe et al., 2014). Measurements of long-lived tracers are the strongest observational constraint on the stratospheric age of air, a key measure of the stratospheric large-scale circulation. Turbulence also modifies the character of kinetic energy fluxes. The magnitude and variability of these energy fluxes determine the rate of frictional dissipation in the atmosphere. This dissipation is represented in global models by a damping parameter and is the primary determinant of the mesoscale atmospheric kinetic energy spectrum. The uncertainty in kinetic spectrum is important to the understanding of the large-scale circulation of the middle atmosphere (Jablonowski & Williamson, 2011).

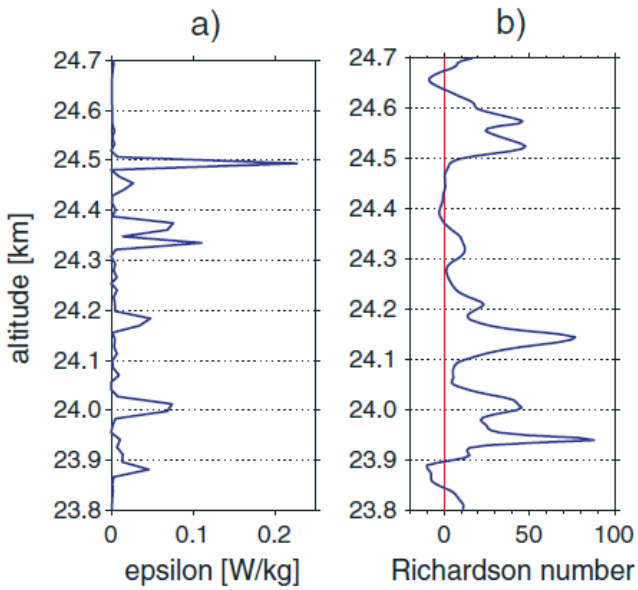

Figure 8: LITOS balloon-borne high-speed anemometer measurements reveal that models of atmospheric turbulence do not explain observed stratospheric turbulence. Physical models predict that a low Richardson number (buoyancy/shear ratio) implies turbulence, but high values of epsilon (turbulent dissipation) should be correlated with low Richardson number, which is not observed. (Haack et al., 2014)

Physical models predict that a low buoyancy/shear ratio (Richardson number) implies turbulence, and that high values of turbulent dissipation should be correlated with low Richardson number (Figure 8). However, recent balloon born measurements during the LITOS campaign did not agree with this, with numerous instances of high values of turbulent dissipation occurring at high Richardson numbers (Haack et al., 2014). As detailed above, both the impact of turbulence on mixing and the associated dissipation of energy are important for general stratospheric science. The point at which viscous fluid forces dominate atmospheric motion is the point where atmospheric motions become purely statistical and is called the dissipation scale. At this scale, models no longer require computationally expensive deterministic modeling. Furthermore, these viscous forces are also responsible for the dissipation of turbulent kinetic energy. Therefore, measurements which resolve the winds at the dissipation scale will allow numerical models to realistically close the atmospheric kinetic energy budget, an important metric of model fidelity.

4.1.2. Importance of Small-Scale Mixing for SAI and SCoPEx

From an SAI and SCoPEx perspective, plume-scale turbulence influences the frequency of collisions of monomer particles within the SCoPEx plume, which determines the rate of formation of fractal, larger aggregates. While Van der Waals forces finally determine whether particles that collide stick together and remain as a fractal aggregate (Sukhodolov et al., 2018), the collision rate is a critical quantity in determining total coagulation rate. Therefore, it is essential to know the frequency of collisions. This frequency is controlled by the wind variability at small spatial scales, i.e., the power spectrum. Intuitively, inertial forcing of particles by wind is much stronger than thermal forcing (e.g. Boltzmann distribution of velocity for ~1 µm particles at ~220 K). Fractal aggregates have a shorter lifetime in the stratosphere and are less effective at scattering light on a per mass basis (Weisenstein et al., 2015), so being able to model the formation

rate of fractal aggregates is an important aspect of SAI, especially with alternate SAI materials.

Improved knowledge of collision rates from wind measurements will allow for the selection of the appropriate mathematical representation of particle coagulation, the coagulation kernel. An accurate kernel is essential for numerical models to correctly simulate aerosol microphysical processes that determine the size distribution and residence time of solid aerosol particles. Adding wind and turbulence measurements to the SCoPEx payload will therefore address the major sources of uncertainty in aerosol microphysics under real atmospheric conditions, which include small-scale fluid flow, particle composition, and humidity.

4.1.3. Experimental Methods to Measure Turbulence in the Stratosphere

Multiple technologies are possible to achieve wind measurements with the necessary spatial resolution under stratospheric conditions. Current state of the art options include pitot tubes (with high sensitivity micro-pirani pressure sensors), hot wire anemometers, and acoustic anemometers. An existing stratospheric program has utilized hot wire anemometers to make measurements that are a close analog to what is necessary for SCoPEx. The program developed LITOS (Leibniz-Institute Turbulence Observations in the Stratosphere), an instrument which made measurements of stratospheric turbulence up to 29 km (Gerding et al., 2009; Theuerkauf et al., 2011). The LITOS instrument has undergone significant calibration and has been compared against radiosondes (Schneider et al., 2015). One drawback of its deployment on a balloon has been the contamination of its wind measurements due to the influence of the balloon's wake. In contrast, SCoPEx is engineered so that the wind environment of the instrument payload is well separated from the balloon wake when SCoPEx is traveling horizontally. For this reason, SCoPEx could provide significantly more data per flight at a chosen float altitude. In this way, SCoPEx and LITOS would be very complementary. The horizontal flight path of SCoPEx, combined with measurements of the wind power spectrum, would provide an excellent complement to the LITOS observations, which are only obtained along a vertical profile. These power spectra obtained by SCoPEx would contribute to improved micrometeorology understanding relevant both to stratospheric aerosol injection and to fundamental atmospheric science.

Additionally, air flow through the turbulence instrument will be simulated using CFD tools. The CFD runs will provide a means to identify key flow characteristics that drive sensor performance (sensitivity and accuracy) and detailed sensor design. This application of the SCoPEx platform would therefore constitute a nonperturbative means to obtain necessary turbulence measurements that have, to date, eluded the scientific community. This information is important for understanding stratospheric dynamics, including the response to climate change or stratospheric heating from SAI. As no injection of particles is needed, these could be among the first scientific measurements to be conducted.

4.2. Goal 2: Evaluation of Aerosol Microphysics of AM-Sulfate and Alternative SAI Materials

One of the goals for which there are insufficient observational analogues is the near-field evolution of particles injected from a point source in the stratosphere. Specifically, observations of the temporal and spatial evolution of the aerosol size distribution (number and volume) of solid, alternate SAI materials or AM-H_2SO_4 injected form a point source can

only be compared with plume model predictions via a perturbative experiment such as SCoPEx. In the following we describe a plume model by Golja et al. (2020) specifically designed for SCoPEx. We also explain the results from the model and the SCoPEx experimental approach for comparing observations with model results.

4.2.1. Plume Model

Golja et al. (2020) incorporated the SCoPEx design features in their model to study the injection of a solid aerosol and vapor-phase sulfuric acid from a balloon payload. To provide observations relevant to SAI, SCoPEx needs to produce downstream aerosols with radii within the range of roughly 0.2 to 1.0 μm. For calcium carbonate, the objective is to maintain a high fraction of the aerosol in monomer form, while for sulfate an ideal distribution would have a peak diameter of 0.6 μm (Dykema et al., 2016). The generation of largely smaller than ideal particles, while imperfect for assessing radiative efficiency relevant to SAI, does not serve to increase particle sedimentation rates within the plume. Such smaller sizes may, however, result in a larger surface to volume ratio, which can strongly influence stratospheric composition as heterogeneous chemistry is directly related to surface area. Distributions centered on small particle sizes in the near field may, however, continue to evolve beyond the domain of the study.

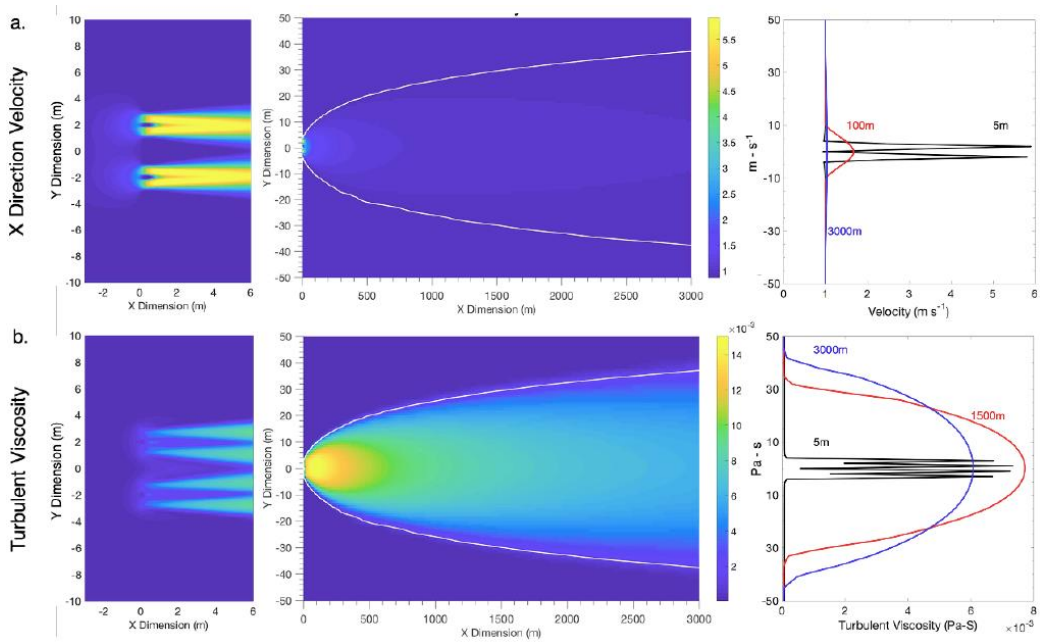

Figure 9 : ANSYS Fluent Velocity and Turbulence Fields. Shown above are the steady state x-direction velocity, u, and turbulent viscosity fields generated by ANSYS Fluent. Left panels show the genesis of disruptions to background X direction flow of 1 ms^{-1}, where propeller features are imposed at locations of 0,2) and (0,-2) meters. The center panel shows the entire domain, from 0 to 3 km, where the imposed red line contours 1 ms^{-1} in plot A, and contours 10% of the absolute maximum turbulent viscosity in plot B. Note Y direction scaling differs between the center and left panels. The right panel shows cross sections of velocity (A) and turbulent viscosity (B) through the Y plane at varying X locations. (Golja et al. 2020)

The velocity and turbulent viscosity fields from Fluent are shown in Figure 9. These fields form the basis of the simulation environment and are instructive in achieving an understanding of SCoPEx and the perturbation it achieves. Peaks in the x-direction velocity, u, are found directly downstream from the modeled propeller centers with an absolute maximum value of 6.3 ms^{-1}. By 1500 m downstream from the inlet locations, the velocity is reduced to the imposed background flow of 1 ms^{-1}. Turbulent viscosity, used as a measure

of particle mixing with background air, exhibits a narrow distribution of peak values ~10 m downstream from simulated propellers. With increasing distance downstream, the turbulent velocity spatial distribution widens, attaining a full width half maximum (FWHM) of 60 m by 1500 m downstream. The wake of the balloon itself is not visible, as it is sufficiently far from the payload to avoid wake crossing/interaction. Additionally, this simulation assumes a laminar stratospheric background flow, neglecting the potential impacts of breaking gravity waves.

For SCoPEx, precipitated calcium carbonate powder with roughly monodisperse size distribution centered at ~0.5 mm diameter will be aerosolized using the expansion of powder suspended in high pressure CO_2 through a 1-2 mm nozzle (see description in Section 3). The model injects aerosol as a 3D gaussian distribution of mass flux into the model grid, where the size of that distribution represents the scale of which the high velocity jet from the nozzle mixes with ambient air. The model considered two injection scenarios: scenario 1 (S1), a single point injection between the propellers; and scenario 2 (S2), injection from the center of each propeller. The model plume diameter at 3 km is, however, insensitive to the injection scenario for injection of both AM-H_2SO_4 and calcium carbonate. This suggests that injection at or between the propellers does not significantly alter the characteristics of the particles' experienced velocity field, and scenario S1 is the one selected for testing the model of plume evolution on SCoPEx. This is also important for the SCoPEx experiment as it necessitates only one sprayer that can be more easily placed in the equipment gondola.

4.2.2. Modelled Mass Injection Rate Dependence of Aerosol Size Distribution

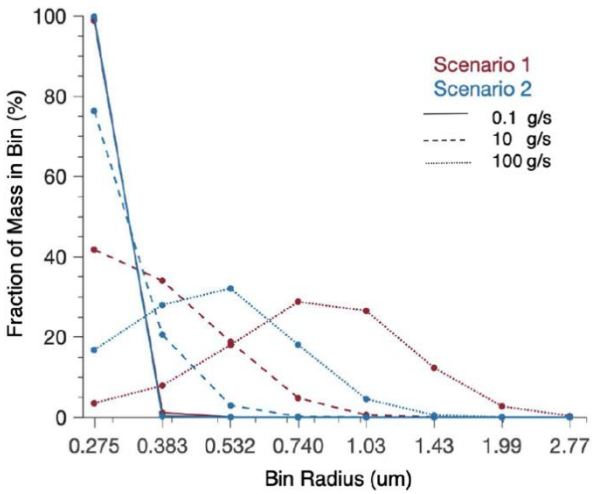

Figure 10: Calcium carbonate aerosol size distributions. Fraction of total mass in each sectional bin where the x-axis markers represent the central radius of each sectional size bin. These distributions represent the percent of total aerosol mass in the final 100 m of the plume across the full domain. Results are shown for three injection rates, 0.1 g s^{-1}, 10 gs^{-1}, and 100 gs^{-1}, for injection scenario 1 (red) and 2 (blue). (Golja et al. 2020)

Mass injection rates of 0.1, 10, and 100 g s^{-1} (0.36, 36, and 360 kg hr^{-1}) were used to test the influence of initial particle number density on the final plume aerosol size distribution. Although some of these are high, their use in the model is instructive as it can answer how different a short burst of high injection rate (much less than an hour) is from a slower but longer injection for the same total mass. Increasing calcium carbonate injection rates from 0.1 to 100 g s^{-1} reduces the share of monomer particles and increases undesired multi-monomer fractal aggregates. Figure 10 shows calcium carbonate's size distribution in the final 100 m of the modeled plume, i.e., the percent in each bin for the three different

injection rates of 0.275 μm radius particles. The low calcium carbonate injection rate of 0.1 g s^{-1} is the most desirable, maintaining 99% of the total mass in the final 100 m of the plume in monomer form. Increasing mass injection rate to 10 g s^{-1} and 100 g s^{-1}, with an S1 injection, shifts peak mass loading to favor particles of radii 0.5 and 0.75 um, respectively, corresponding to fractal "dimers" and "trimers".

Golja et al. (2020) also evaluated whether, in addition to the very sensitive in-situ optical particle counting aerosol size distribution instrument which originally was designed to measure background stratospheric aerosol size distributions (Murphy et al., 2016), the plumes could also be detected optically via scattered light. It should be emphasized that this does not refer to measurements from the ground but rather from close to the plume, e.g., when the equipment gondola is in close vicinity to the plume. Measuring the scattering from one view angle gives the product of the scattering phase at that angle and the scattering efficiency. This is closely related to the radiative forcing, but it does not uniquely determine the radiative forcing. By measuring at multiple angles, we could obtain enough information to quantify the radiative forcing. For example, we could measure from the side and below to obtain the forward scatter fraction, then calculate backscatter by flux conservation.

In the model, the extinction optical depth was calculated using Mie scattering theory and vertically integrating down columns in the y-z plane. Figure 11 shows the relative optical thickness of a sulphate and calcite aerosol plume formed via scenario 1 with an injection rate of 0.1 g s^{-1}. Calcite exhibits greater optical thickness by an order of magnitude at 550 nm, with an average value of 8.6×10^{-4} and maximum of 0.014 across the domain, as compared to sulphate, with an average of 9.4×10^{-5} and maximum 0.001. From these values, Golja et al. calculated that we expect adequate SNR to confidently detect the plume with a fast-scanning radiometer via the solar radiation it scatters. This calculation assumed an altitude of 21 km, solar elevation angle of 60°, an observing instrument situated on the payload gondola, and the gondola 200 m away from the edge of the plume and 1 km downstream of the termination of a scenario 1 type injection of calcite aerosol. Details of this calculation can be found in Golja et al. (2020).

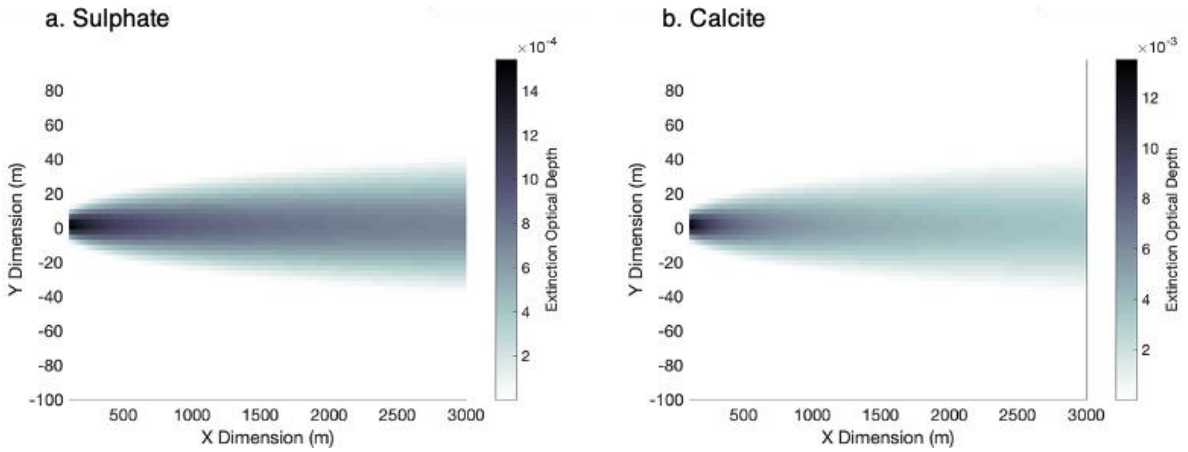

Figure 11: Extinction optical depth integrated vertically through all columns in the plume from 100-3000 m. Plots a and b show results for 0.1 gs^{-1} injections of condensable H_2SO_4 and calcite, respectively. The resulting number density of calcite aerosol is 490 cm^{-3} on the centerline at a downstream distance of 1000 m, predominantly as monomers. Aerosol optical depths were derived from Mie scattering theory at 550 nm, using refractive indices for sulphate and calcite stated in Dykema et al. (2016). (Golja et al. 2020)

4.2.3. SCoPEx Experimental Design and Analysis of Plume Evolution

For this goal, SCoPEx will follow the standard concept of operations, first spraying calcium carbonate at an injection rate suggested by the model analysis. It is desirable to maximize the contrast with the background stratosphere, both with respect to the aerosol concentration and the potential resulting chemical changes, while also maintaining calcium carbonate as monodisperse aerosol. To this end, additional models will be run at injection rates between 0.1 and 10 gs^{-1}. Based on these results, an injection rate will be chosen for the actual SCoPEx experiment. In addition to the basic components of the SCoPEx platform (gondola, ascender, propulsion, power, flight computer, communication, and wind), the calcium carbonate sprayer as well as the LIDAR and POPS instrument are critical for this science goal; without these components, there would not be a way to make and find the plume or measure the aerosol size distribution. While the turbulence measurement from goal 1 is desirable, it is, at least initially, not necessary. Similar studies of AM-H_2SO_4 injection would also be extremely useful. Our current plan is to conduct these after the calcium carbonate injection studies, as initially calcium carbonate is easier to handle than sulfuric acid and its precursors (see next section for motivation of calcium carbonate).

The aerosol size distribution measurements will be compared with the model predictions. In combination with turbulence measurements, discrepancies between the observed and modeled aerosol size distributions can be used to identify issues within the aerosol microphysical scheme or highlight misrepresentations of the velocity and turbulence field of the payload. The results of these studies will provide critical observational constraints on the aerosol microphysics and plume evolution of an injection with solid particles. It will be unique data that is ideal for testing the model of plume evolution as SCoPEx does not have to address problems resulting from the much more violent injection regime associated with injection from airplanes. Clearly, such studies are also needed, but SCoPEx represents a feasible and compelling first step in a sequence of new studies that more comprehensively investigate the aerosol microphysics of point source injections.

4.3. Goal 3: Evaluation of Process Level Chemical Models of Stratospheric Chemistry of Sulfate and Alternative SAI Materials

4.3.1. Need for Alternative SAI Materials

As previously discussed, the two largest first-order stratospheric risks of SAI with sulfate aerosol are ozone depletion and stratospheric heating. For sulfate aerosol the relative magnitude of these two risks can be adjusted if the size distribution can be controlled, e.g., via the AM-H_2SO_4 approach. It is worth noting that the impact on stratospheric ozone may be greatly reduced in the future if reactive halogen concentrations are lower. In contrast, the impact of stratospheric heating will not change. This represents a risk with a poorer understanding of its consequences, which makes it highly desirable to minimize stratospheric heating and resulting dynamic response. Therefore, it is important to investigate alternative SAI materials.

The properties of the “ideal” SAI material is (i) no absorption of radiation, i.e., purely scattering aerosol both fresh and aged, (ii) chemically inert, i.e., no direct impact of this material on stratospheric composition, and (iii) minimal down-stream effects, i.e., no impact on cirrus or other clouds, no environmental impact on deposition on the ground, etc. In reality, it is unlikely that a material with no impacts exists and rather the question is which materials can minimize these impacts. There have been a number of studies investigating

SAI materials in this context. High refractive index materials have been suggested as they reduce the mass of material that have to be lofted (Ferraro et al., 2015; Ferraro et al., 2011; Pope et al., 2012; Keith et al., 2016; Dai et al., 2020; Weisenstein et al., 2015). This largely cost-driven perspective is not a motivation for our work. In contrast, one of the goals of SCoPEx is to decrease the uncertainty in SRM models that use calcium carbonate SAI. The rationale for the choice of calcium carbonate as well as the approach to evaluate some of these risks is described in the following sections.

4.3.2. Unreactive Alternative SAI Materials

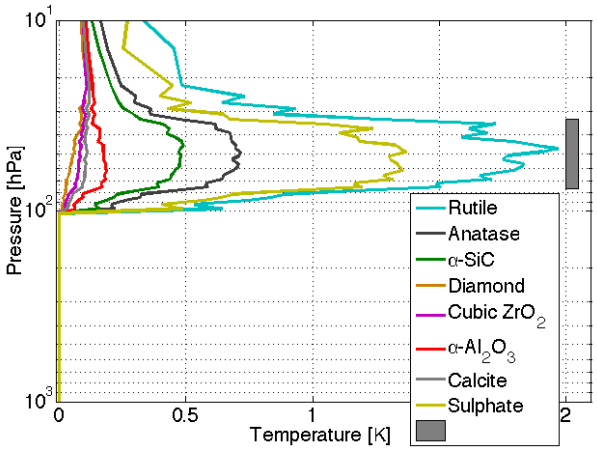

Figure 12: Comparison of stratospheric heating for different materials. Diamond has the lowest impact, although cubic zirconia and calcite are very similar. Sulfate and rutile result in much larger heating. (Dykema et al., 2016)

Diamond is probably the material with the best properties for SAI from a purely stratospheric perspective. Diamond has no absorption features in the solar or terrestrial spectrum and thus triggers the minimal possible dynamical response Figure 12. In addition, diamond should have ideal chemical properties. Hydrogen-terminated diamond surfaces are extremely inert and hydrophobic, precluding the ozone destroying chemistry initiated on sulfuric acid surfaces. The surface itself is also resistant to concentrated sulfuric acid. Exposure to OH radicals would probably slowly make the surface more hydrophilic. From a purely stratospheric perspective the only first-order risk of diamond would be increased ozone loss from the increased sulfuric acid surface area resulting from coagulation with background sulfate aerosol.

4.3.3. Reactive Alternative SAI Materials: The Case for Calcium Carbonate

Although the impact on cloud properties and the risk to Earth's surface from deposition of SAI diamond is likely very low, it could be preferable to have a material that dissolved easily in water, hence not persisting for long times outside of the stratosphere. It would also be preferable to have a material that is naturally abundant at Earth's surface. In addition, it would be ideal to overcome increased ozone loss due to coagulation by using a reactive aerosol. We therefore propose calcium carbonate as a prototype alternate SAI material for the following reasons: First, its optical properties are nearly equal to diamond and stratospheric heating and resulting dynamic response should be negligible compared to sulfate (Figure 12). Second, carbonates are typically quite reactive with acids, especially with concentrated sulfuric acid (Figure 13). Hence, calcium carbonate will neutralize upon

coagulation with sulfate aerosol eliminating the acidic surfaces resulting from coagulation of diamond and sulfate aerosol. Of course, the reactivity of calcium carbonate also makes model predictions with calcium carbonate more complex. The evolution of chemical and optical aerosol properties has to be modeled over its stratospheric lifetimes. One of the key research questions that SCoPEx will help address is whether the reactivity of calcium carbonate and the evolution of its chemical and optical properties and those of the surrounding gas-phase correspond to the detailed hypothesis laid out below. To this end, SCoPEx will compare observations of the chemical evolution of calcium carbonate, as well as the gas-phase, with those of a model based on known properties of calcium carbonate and recent laboratory experiments (Dai et al., 2020). This will provide a real-world evaluation of kinetic parameters, such as heterogeneous uptake coefficients derived from the laboratory studies, that will enable GCMs to include reliable parameterizations of the stratospheric impacts of calcium carbonate SAI.

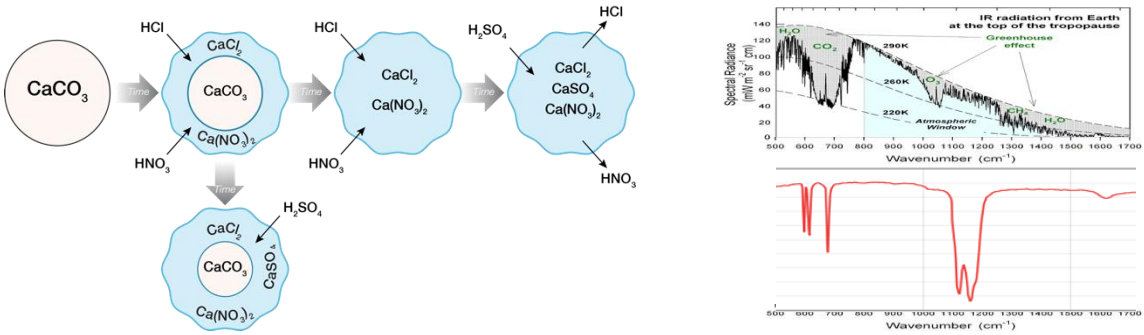

Figure 13: The left panel shows schematic of potential chemical reactivity of calcium carbonate in the stratosphere. The right panel shows the atmospheric windows in the terrestrial infrared (top) as well as the infrared absorption spectrum of calcium sulfate (bottom). The position of the 1150 cm^{-1} sulfate in part explains the stratospheric heating effect of sulfuric acid.

4.3.3.1. Optical Properties

Based on well-established chemistry, the reaction of sulfuric acid aerosol with calcium carbonate can be assumed to go to completion, i.e., be reagent limited. The optical properties of calcium sulfate in the terrestrial infrared are similar to those of sulfuric acid with only slight differences in relative band intensities and wavelengths (Figure 13 right hand inset). This is important as it implies that there will be no large first-order changes in stratospheric heating from changing background sulfuric acid to calcium sulfate. There are higher order impacts due to slight differences in the absorption of sulfuric acid, which has some liquid water compared to calcium sulfate. There are also numerous forms of calcium sulfate (anhydrite, bassanite, gypsum, etc.). However, the resulting differences are much smaller than introducing an absorbing material via SAI.

4.3.3.2. Chemical Properties

Predicting the evolution of the chemical properties of calcium carbonate under stratospheric conditions is more challenging. It is certain that calcium carbonate does not have the same heterogeneous reactions that activate ozone destroying substances as sulfuric acid. Figure 13 shows a schematic of the expected reactivity. Calcium carbonate is expected to react with acidic substances neutralizing them, forming salts and carbon dioxide. These acid neutralizing reactions can deplete gas-phase HNO_3, HCl, etc. There are a large number of ozone destroying catalytic cycles involving NOx, chlorine and other

halogens, which are altitude (and latitude) dependent. NOx can be produced via HNO_3 photolysis and lost via heterogeneous reaction of N_2O_5. It participates both in ozone destroying catalytic cycles and is important for deactivation of ozone destroying halogen radicals. Thus, knowledge of the heterogeneous reaction rates of numerous substances with calcium carbonate are required to predict the impact it will have on stratospheric composition.

However, until the recent study by Dai et al. in our laboratory, no heterogeneous chemistry studies of calcium carbonate under stratospheric conditions had been conducted, to our knowledge, although there exists a rich data set under tropospheric conditions (Dai et al., 2020). This work, as well as the work of Dai et al., highlights that reactive solid aerosols are indeed more complex than liquid sulfuric acid: The authors observed moderate initial uptake of the gas-phase acids HCl and HNO_3 on fresh calcium carbonate, as the dry stratospheric conditions already make uptake coefficients lower than under typical tropospheric conditions. An additional large difference to liquid aerosol is that the surface of the solid calcium carbonate passivates, drastically reducing the uptake coefficients of HCl and HNO_3. Hence, based on the Dai et al. laboratory study, calcium carbonate rapidly becomes effectively unreactive with respect to uptake of these gas-phase acids, an important finding that confirms calcium carbonate as a good candidate as alternate SAI material. In addition, calcium carbonate particles are abundant at Earth's surface due to windblown mineral dust. And the small calcium carbonate SAI particles should dissolve rapidly in water. This does not exclude risks associated with the deposition of calcium carbonate SAI particles or impacts on clouds (Cziczo et al., 2019). However, due to its abundance at the Earth's surface, there already exists a large knowledge base for its environmental impacts in contrast to, e.g., diamond. Further laboratory work is required to study especially the $ClONO_2$ + HCl and N_2O_5 hydrolysis reactions on fresh and aged calcium carbonate. However, the existing results prepare the stage for studying them in the real stratospheric environment as outlined below. Figure 14 shows results of the AER 2-D chemistry-transport-aerosol model for annual average ozone column changes of calcium carbonate SAI compared to a control for 2040. Ignoring the passivation of calcium carbonate (thk-ind) results in increases in ozone columns from calcium carbonate SAI whereas the inclusion of passivation can either result in very little ozone column change or losses in the Southern Hemisphere, depending how the $ClONO_2$+HCl is parameterized. Either of the two, more realistic, passivation scenarios result in significantly lower ozone loss than the equivalent amount of sulfate SAI, consistent with the hypothesis.

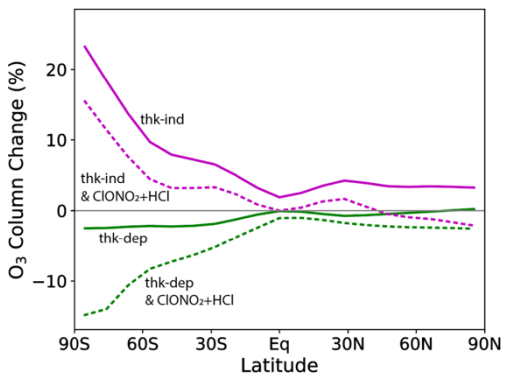

Figure 14: Shows the role of passivation and the heterogeneous $ClONO_2$+HCl reaction on ozone column change using the AER 2-D model taken from Dai et al. 2020. Inclusion of this reaction with the same rate as measured for Al_2O_3 results in a substantial reduction in ozone for scenarios including, thk-ind, or excluding passivation, thk-dep.

4.3.4. Need for SCoPEx Calcium Carbonate Plume Studies

One of the challenges for alternate SAI aerosol is the lack of materials such as calcium carbonate in the stratosphere. The only way to then study these materials in the actual stratosphere is via deliberate stratospheric injection of a small amount of these materials. In environmental studies, including stratospheric studies, it is not possible to rely purely on laboratory studies. For example, flights on the NASA ER-2 into the polar vortex over Antarctica provided the ability to test whether laboratory-derived reaction mechanisms were able to capture real-world ozone destruction chemistry. Without these flights, the level of confidence in the model predictions would have been much lower, and for good reason. It is not clear that a given experimental setup in the laboratory can faithfully capture the entire complexity of the real stratosphere; only field observations are able to provide this. For a number of natural stratospheric processes, remote observations can provide important information in addition to in situ aircraft or balloon. However, these are only possible when large-scale phenomena are at work.

Since there are no natural calcium carbonate plumes in the stratosphere that would even allow for in situ observations, intentional injection is necessary to perform these studies. Calcium carbonate injections will allow SCoPEx to provide invaluable observations as it will quantitively test the mechanisms determined in the laboratory. As stated above, there is a need for more laboratory studies, however, there is good reason to proceed with the planning of SCoPEx calcium carbonate experiments. First, by the time of the first injection experiments, additional studies should have been conducted. In addition, N_2O_5 uptake coefficients used in the model are likely a very good estimation as similar values have been found for different solid materials, e.g., Al_2O_3 and SiO_2 (Molina et al., 1997). In addition, even with these additional lab determined mechanisms, the same type of experiments as proposed here will still have to be conducted, as we expect these reactions to not make a significant difference. In other words, they will not be a deciding factor about the viability of calcium carbonate as an alternate SAI material. Only field experiments will help shed insight into these questions. In summary, there is a critical need for evaluating not just the aerosol microphysics (goal 2) but also the stratospheric chemistry of calcium carbonate due to the promise it holds as a lower risk SAI material.

4.3.5. SCoPEx Experimental Design and Analysis of Chemical Calcium Carbonate Plume Evolution

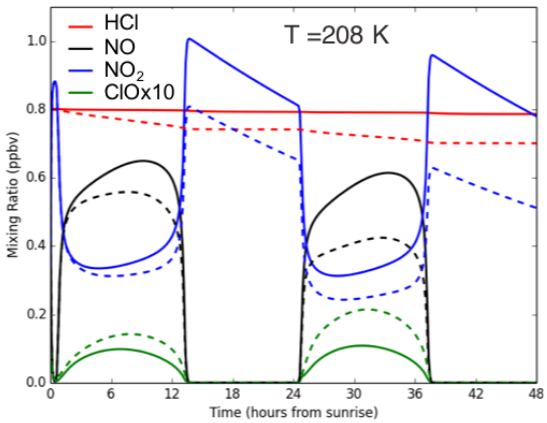

Figure 15: Solid lines: background 2μm^2 cm^{-3} sulfate 5ppm$_v$ H_2O. Dashed lines: plume 15μm^2 cm^{-3} sulfate 10 ppm$_v$ H_2O.

The experiments will again follow the standard concept of operations as under goal 2. In order to determine optimal injection rates, we will include chemical reactions in the plume model, updated with the newest mechanisms available at that time. Figure 15 shows the evolution of an air mass perturbed by a sulfate aerosol injection over multiple days, i.e., significantly longer than the initial SCoPEx experiments. Significant changes in HCl and NOx can be observed already over short time periods and these are easily detectable with existing instrumentation. For this science goal, it is desirable to measure aerosol composition and size distribution as well as key gas-phase chemical species, especially HCl, NOx and water. Therefore, this science goal requires a much larger set of instruments. In addition, the equivalent model to Figure 15 for calcium carbonate is informed by the results of science goal 2. The work of Dai et al. provides kinetic parameters needed for this model, and reactions for which there are no laboratory data to date are parameterized using close analogues and conditions, e.g., $ClONO_2$ + HCl are parameterized using the results for alumina (and silica) from Molina et al. (1997). One key question is whether the changes in HCl and NOx will indeed be smaller for calcium carbonate than those for sulfate shown in the figure above, which would confirm the hypothesis for calcium carbonate as a potential alternate SAI material.

In summary, SCoPEx experiments using calcium carbonate injections will provide a unique evaluation as to whether calcium carbonate indeed is an alternate SAI material that could substantially reduce risk from SAI compared to sulfate. Follow-up studies will be needed. For example, improved chemical and aerosol microphysics models will provide improved models of the chemical and physical evolution of calcium carbonate, which likely will motivate specific laboratory investigations. These will provide information for SCoPEx studies using “stratospherically aged” calcium carbonate as precursor for injection that can then be used to compare whether the laboratory mechanisms of this aged calcium carbonate agree with that found in the real stratospheric environment.

5. Data Management Plan and Dissemination of Results

Products of the research. The data generated during this project consists of meteorological, navigational, telemetry, and a variety of instrumentation data, in particular aerosol size distributions as well as chemical composition data during later science flights. In addition, there will be model data on plume chemical evolution.

Access to data, data sharing practices, and policies and dissemination of results. Data relevant for scientific analysis will be made public within 60 days of the end of flight. This taw data will be made public with appropriate warnings that it has not undergone QA/QC. The email address of users will be recorded so that they can be automatically notified when revised versions become available. Based on previous experiences with stratospheric airborne campaigns, this is typically 6-15 months after the flight depending on the type of data, e.g., the amount of calibration and data workup required. We have chosen to make raw data available rapidly—going far beyond what is typical for stratospheric science missions—because of the public scrutiny of SCoPEx and because of the broad commitment to Open Access data principles articulated by Harvard's Solar Geoengineering Research Program which is funding SCoPEx.

Principal Investigators (PI) and their groups have an excellent track record with presenting their work at major national and international conferences and workshops. All data that go into key analyses and figures in the group's publications will be made publicly available via the PI's group website. All publications resulting from this project will be posted on the PI's webpage (https://projects.iq.harvard.edu/keutschgroup/publications). Preprints of manuscripts submitted for publication as well as the underlying data will also be posted on Harvard's Dash manuscript repository. Publications will be made in open access formats.

Archiving of data. All data acquisition/storage computers in the PI's group are automatically backed up daily, both wirelessly to a server elsewhere on campus, and/or to a cloud server. Both of these processes ensure that data will not be lost and enable rapid access to the data. The file naming system used for all software (which includes the date of the experiment) ensures straightforward retrieval and use of archived data. Group laptops are also backed up daily, ensuring that analyzed data are archived as well.

6. SCoPEx Research Team Biographies

Frank Keutsch was born in Tübingen, Germany and received his Diplom in chemistry from the Technische Universität München, Germany, under the supervision of Vladimir E. Bondybey in 1997. He received his PhD in physical chemistry from the University of California at Berkeley in 2001. His graduate research was conducted under the direction of Richard J. Saykally and focused on vibration−rotation−tunneling spectroscopy and hydrogen-bond-breaking dynamics in water clusters. After working on stratospheric chemistry in the Department of Chemistry and Chemical Biology at Harvard University under the direction of James G. Anderson, he started his independent academic career in 2005 at the University of Wisconsin-Madison. He then moved to his current position as Stonington Professor of Engineering and Atmospheric Science at Harvard University in the Paulson School of Engineering and Applied Sciences and the Department of Chemistry and Chemical Biology and he has held numerous visiting professor positions. Keutsch Group research combines laboratory and field experiments with instrument development to investigate fundamental mechanisms of anthropogenic influence on atmospheric composition within the context of impacts on climate, humans and the environment. Keutsch's main focus has been on understanding how *unintentional* emissions of pollutants such as nitrogen oxides, sulfur dioxide, and hydrocarbons have changed key chemical pathways controlling ozone and particulate matter, two key pollutants affecting human health and climate. Keutsch has been the PI of numerous research grants for this research and currently is the deputy-PI for the NASA-EVS3 DCOTSS campaign. Keutsch has also been focusing on improving the understanding of how *intentional* emissions within the context of stratospheric solar radiation modification could impact the protective stratospheric ozone layer and stratospheric dynamics and climate, and how known risks can be better quantified or reduced. He is currently the PI of SCoPEx. Keutsch has received awards for his teaching, which spans a wide range of courses including introductory chemistry, engineering design and atmospheric chemistry.

David Keith has worked near the interface between climate science, energy technology, and public policy since 1991. He received his B.Sc. in physics from the University of Toronto in 1986 and received his PhD in experimental physics from the Massachusetts Institute of Technology in 1991 under the supervision of David Prichard. He took first prize in Canada's national physics prize exam, won MIT's prize for excellence in experimental physics, and was one of TIME Magazine's Heroes of the Environment. David is Professor of Applied Physics at the Harvard School of Engineering and Applied Sciences and Professor of Public Policy at the Harvard Kennedy School, and founder of Carbon Engineering, a Canadian company developing technology to capture CO_2 from ambient air to make carbon-neutral hydrocarbon fuels. Best known for his work on the science, technology, and public policy of solar geoengineering, David led the development of Harvard's Solar Geoengineering Research Program, a Harvard-wide interfaculty research initiative. His work has ranged from the climatic impacts of large-scale wind power to an early critique of the prospects for hydrogen fuel. David's hardware engineering work includes the first interferometer for atoms, a high-accuracy infrared spectrometer for NASA's ER-2, and the development of Carbon Engineering's air contactor and overall process design. On SCoPEx, he is the faculty lead for platform design and engineering. David teaches science and technology policy, climate science, and solar geoengineering. He has reached students worldwide with an edX

energy course. David is author of >200 academic publications with total citation count of >15,000. He has written for the public in op-eds and *A Case for Climate Engineering*. David splits his time between Cambridge, Massachusetts and Canmore, Alberta.

Norton Allen is Head Software Engineer for the Anderson, Keith, and Keutsch groups in the Harvard John A. Paulson School of Engineering and Applied Sciences. Working closely with electrical and mechanical engineering, he is responsible for the design and deployment of software for data acquisition and control on all flight instruments. He has successfully deployed over two dozen instruments and supported field deployments in locations around the world. He received an AB cum laude from Harvard College, studying math, applied math, computer science, and physics.

John Dykema is a Project Scientist at the Harvard John A. Paulson School of Engineering and Applied Sciences and the LIDAR principal investigator on SCoPEx. His main interests are atmospheric radiation and remote sensing instrumentation, with an emphasis on development of novel, compact LIDARS for trace gas and aerosol measurement. John earned his AB in physics from UC Berkeley and his PhD in applied physics from Harvard University, where his dissertation focused on developing a new airborne infrared sounder that was a prototype for a climate-focused atmospheric radiation mission. He is participating in the NASA DCOTSS mission as the principal investigator for the POPS optical particle counter and as a member of the DCOTSS aerosol science subgroup. He also collaborates with several external organizations in designing and simulating new LIDAR prototypes, incorporating emerging laser and optical technology. John leads the engineering development and data analysis for the SCoPEx LIDAR and works on the radiative and micrometeorological science aspects of the SCoPEx mission.

Mike Greenberg is the Lead Optical-Mechanical engineer for the Anderson, Keith, and Keutsch groups in the Harvard John A. Paulson School of Engineering and Applied Sciences. He is responsible for the mechanical development and implementation of flight and laboratory based instrumentation, equipment packaging, documentation, and platform integration. Working closely with the electrical, software, and science team members, he has over 20 years of experience developing, delivering, and supporting designs and has been on more than a dozen airborne campaigns with the ER-2, WB-57, and DA-42 aircraft platforms and with stratospheric balloons. Mike received a BSME from Tufts University and a MSME from Stanford University. His additional work experiences include time spent Argonne National Laboratory and The Raytheon Company.

Michael Litchfield is the Senior Engineering Lead for Climate Research in the Anderson, Keith, Keutsch groups at the Harvard John A. Paulson School of Engineering and Applied Sciences and the engineering lead on the SCoPEx Flight Platform development program. He and the rest of the engineering team are focused on taking high level SCoPEx flight platform requirements through the design, fabrication, assembly, test, and validation processes. Michael earned his BS and MS degrees in Electrical Engineering specializing in controls and communications systems at Worcester Polytechnic Institute. Prior to joining the lab to assume this role, Michael worked for over 30 years in industry across 5 start-ups leading their various engineering teams in bringing first products to market where those markets included; X-ray Semiconductor Lithography, 3D Ultrasound

Medical imaging , X-ray 2D Projection / 3D CT Airport Baggage Security Imaging, and 4D (3D movies) mmWave Personnel Security imaging.

Craig Mascarenhas is a mechanical engineer for the Anderson, Keith, and Keutsch groups in the Harvard John A. Paulson School of Engineering and Applied Sciences. He is responsible for the mechanical design and integration of instrumentation, equipment packaging, and aerodynamic analysis of flight systems. He has previously been involved in instrument design for airborne campaigns with the ER-2 and stratospheric balloons. Craig received a BASc from the University of Toronto and an SM from MIT. His additional work experiences include engineering roles in the nuclear, biotech, and hydro-power industries.

Terry Martin is an electronics technician with the Anderson, Keith, and Keutsch research groups. She has worked on electrical build up and documentation of numerous scientific experiments over the course of the 42 years she has been with the group and is presently helping with the electronic assembly and wiring of the SCoPEx instrument.

Marco Rivero is a senior Electrical Engineer in the Anderson, Keith, and Keutsch groups in the Harvard John A. Paulson School of Engineering and Applied Sciences. As such, he has been primarily involved in the electrical engineering design, fabrication, and testing of the SCoPEx platform and payload instrumentation since inception. Marco holds a BS in Microelectronic Engineering from Rochester Institute of Technology and a MS in Electrical Engineering from Tufts University. During his 25 years with the group, Marco has been involved in the electronics and systems design of 14 airborne instruments and supported their deployment in over 20 NASA national and international field campaigns; most recently, a HCl instrument deployment out of NASA's Columbia Scientific Balloon Facility in Fort Sumner NM in August of 2018.

Yomay Shyur is a Postdoctoral Fellow at the Harvard John A. Paulson School of Engineering and Applied Sciences and a project manager and project scientist on SCoPEx. She leads technical project coordination, works on science instrument design and analysis, and assists with platform engineering tasks. Yomay earned her BA in physics from Wellesley College and her PhD in physics from the University of Colorado Boulder, where her dissertation focused on developing new experimental methods of manipulating cold molecules using high-voltage electrodes and laser detection techniques.

References

Anderson, M. R., Miake-Lye, R. C., Brown, R. C., & Kolb, C. E. (1996). Calculation of exhaust plume structure and emissions of the ER 2 aircraft in the stratosphere. *Journal of Geophysical Research: Atmospheres*, *101*(D2), 4025–4032. https://doi.org/10.1029/95JD02366

Bala, G., Duffy, P. B., & Taylor, K. E. (2008). Impact of geoengineering schemes on the global hydrological cycle. *Proceedings of the National Academy of Sciences*, *105*(22), 7664–7669. https://doi.org/10.1073/pnas.0711648105

Balluch, M. G., & Haynes, P. H. (1997). Quantification of lower stratospheric mixing processes using aircraft data. *Journal of Geophysical Research: Atmospheres*, *102*(D19), 23487–23504. https://doi.org/10.1029/97JD00607

Benduhn, F., Schallock, J., & Lawrence, M. G. (2016). Early growth dynamical implications for the steerability of stratospheric solar radiation management via sulfur aerosol particles. *Geophysical Research Letters*, *43*(18), 9956–9963. https://doi.org/10.1002/2016GL070701

Butchart, N., Anstey, J. A., Hamilton, K., Osprey, S., McLandress, C., Bushell, A. C., Kawatani, Y., Kim, Y.-H., Lott, F., Scinocca, J., Stockdale, T. N., Andrews, M., Bellprat, O., Braesicke, P., Cagnazzo, C., Chen, C.-C., Chun, H.-Y., Dobrynin, M., Garcia, R. R., … Yukimoto, S. (2018). Overview of experiment design and comparison of models participating in phase 1 of the SPARC Quasi-Biennial Oscillation initiative (QBOi). *Geoscientific Model Development*, *11*(3), 1009–1032. https://doi.org/10.5194/gmd-11-1009-2018

Conway, J. P., Bodeker, G. E., Waugh, D. W., Murphy, D. J., Cameron, C., & Lewis, J. (2019). Using Project Loon Superpressure Balloon Observations to Investigate the Inertial Peak in the Intrinsic Wind Spectrum in the Midlatitude Stratosphere. *Journal of Geophysical Research: Atmospheres*, *124*(15), 8594–8604. https://doi.org/10.1029/2018JD030195

Crutzen, P. J. (2006). Albedo Enhancement by Stratospheric Sulfur Injections: A Contribution to Resolve a Policy Dilemma? *Climatic Change*, *77*(3), 211. https://doi.org/10.1007/s10584-006-9101-y

Cziczo, D. J., Wolf, M. J., Gasparini, B., Münch, S., & Lohmann, U. (2019). Unanticipated Side Effects of Stratospheric Albedo Modification Proposals Due to Aerosol Composition and Phase. *Scientific Reports*, *9*(1), 18825. https://doi.org/10.1038/s41598-019-53595-3

Dai, Z., F. Keutsch, D. Weisenstein, and D. W. Keith. (2020). Experimental reaction rates constrain estimates of ozone response to calcium carbonate geoengineering, *Manuscript submitted for publication.*

Dykema, J., Keith, D., Anderson, J. G., & Weisenstein, D. (2014). Stratospheric controlled perturbation experiment (SCoPEx): A small-scale experiment to improve understanding of the risks of solar geoengineering. *Philosophical Transactions of the Royal Society A*, *372*. https://doi.org/10.1098/rsta.2014.0059

Dykema, J., Keith, D., & Keutsch, F. (2016). Improved aerosol radiative properties as a foundation for solar geoengineering risk assessment. *Geophysical Research Letters*. http://onlinelibrary.wiley.com/doi/10.1002/2016GL069258/full

Fahey, D. W., Keim, E. R., Boering, K. A., Brock, C. A., Wilson, J. C., Jonsson, H. H., Anthony, S., Hanisco, T. F., Wennberg, P. O., Miake-Lye, R. C., Salawitch, R. J., Louisnard, N., Woodbridge, E. L., Gao, R. S., Donnelly, S. G., Wamsley, R. C., Del Negro, L. A., Solomon, S., Daube, B. C., … Chan, K. R. (1995a). Emission Measurements of the Concorde Supersonic Aircraft in the Lower Stratosphere. *Science*, *270*(5233), 70–74.

Fahey, D. W., Keim, E. R., Woodbridge, E. L., Gao, R. S., Boering, K. A., Daube, B. C., Wofsy, S. C., Lohmann, R. P., Hintsa, E. J., Dessler, A. E., Webster, C. R., May, R. D., Brock, C. A., Wilson, J. C., Miake-Lye, R. C., Brown, R. C., Rodriguez, J. M., Loewenstein, M., Proffitt, M. H., … Chan, K. R. (1995b). In situ observations in aircraft exhaust plumes in the lower stratosphere at midlatitudes. *Journal of Geophysical Research: Atmospheres*, *100*(D2), 3065–3074. https://doi.org/10.1029/94JD02298

Farquhar, G. D., & Roderick, M. L. (2003). Pinatubo, Diffuse Light, and the Carbon Cycle. *Science*, *299*(5615), 1997–1998. https://doi.org/10.1126/science.1080681

Ferraro, A. J., Charlton-Perez, A. J., & Highwood, E. J. (2015). Stratospheric dynamics and midlatitude jets under geoengineering with space mirrors and sulfate and titania aerosols. *Journal of Geophysical Research: Atmospheres*, *120*(2), 414–429. https://doi.org/10.1002/2014JD022734

Ferraro, A. J., Highwood, E. J., & Charlton-Perez, A. J. (2011). Stratospheric heating by potential geoengineering aerosols. *Geophysical Research Letters*, *38*(24). https://doi.org/10.1029/2011GL049761

Gao, R. S., Telg, H., McLaughlin, R. J., Ciciora, S. J., Watts, L. A., Richardson, M. S., Schwarz, J. P., Perring, A. E., Thornberry, T. D., Rollins, A. W., Markovic, M. Z., Bates, T. S., Johnson, J. E., & Fahey, D. W. (2016). A light-weight, high-sensitivity particle spectrometer for PM2.5 aerosol measurements. *Aerosol Science and Technology*, *50*(1), 88–99. https://doi.org/10.1080/02786826.2015.1131809

Gerding, M., Theuerkauf, A., & Suminska, O. (2009). Balloon-borne hot wire anemometer for stratospheric turbulence soundings. *Proceedings of the 19th ESA Symposium on European Rocket and Balloon Programmes and Related Research, SP-671*.

Golja, C. M., L. W. Chew, J. A. Dykema, and D. W. Keith. (2020). Aerosol Dynamics in the Near Field of the SCoPEx Stratospheric Balloon Experiment, *Manuscript submitted for publication.*

Gu, L., Baldocchi, D. D., Wofsy, S. C., Munger, J. W., Michalsky, J. J., Urbanski, S. P., & Boden, T. A. (2003). Response of a Deciduous Forest to the Mount Pinatubo Eruption: Enhanced Photosynthesis. *Science*, *299*(5615), 2035–2038. https://doi.org/10.1126/science.1078366

Gu, L., Baldocchi, D., Verma, S. B., Black, T. A., Vesala, T., Falge, E. M., & Dowty, P. R. (2002). Advantages of diffuse radiation for terrestrial ecosystem productivity. *Journal of Geophysical Research: Atmospheres*, *107*(D6), ACL 2-1-ACL 2-23.

https://doi.org/10.1029/2001JD001242

Haack, A., Gerding, M., & Lübken, F.-J. (2014). Characteristics of stratospheric turbulent layers measured by LITOS and their relation to the Richardson number. *Journal of Geophysical Research: Atmospheres*, *119*(18), 10,605-10,618. https://doi.org/10.1002/2013JD021008

Haynes, P. H. (2005). Transport and Mixing in the Atmosphere. In W. Gutkowski & T. A. Kowalewski (Eds.), *Mechanics of the 21st Century* (pp. 139–152). Springer Netherlands. https://doi.org/10.1007/1-4020-3559-4_8

Holben, B. N., Eck, T. F., Slutsker, I., Tanré, D., Buis, J. P., Setzer, A., Vermote, E., Reagan, J. A., Kaufman, Y. J., Nakajima, T., Lavenu, F., Jankowiak, I., & Smirnov, A. (1998). AERONET—A Federated Instrument Network and Data Archive for Aerosol Characterization. *Remote Sensing of Environment*, *66*(1), 1–16. https://doi.org/10.1016/S0034-4257(98)00031-5

Homeyer, C. R., Bowman, K. P., Pan, L. L., Atlas, E. L., Gao, R.-S., & Campos, T. L. (2011). Dynamical and chemical characteristics of tropospheric intrusions observed during START08. *Journal of Geophysical Research: Atmospheres*, *116*(D6). https://doi.org/10.1029/2010JD015098

Hoppe, C. M., Hoffmann, L., Konopka, P., GrooÃ, J.-U., Ploeger, F., Günther, G., Jöckel, P., & Müller, R. (2014). The implementation of the CLaMS Lagrangian transport core into the chemistry climate model EMAC 2.40.1: Application on age of air and transport of long-lived trace species. *Geoscientific Model Development*, *7*(6), 2639–2651. https://doi.org/10.5194/gmd-7-2639-2014

Jablonowski, C., & Williamson, D. L. (2011). The Pros and Cons of Diffusion, Filters and Fixers in Atmospheric General Circulation Models. In P. Lauritzen, C. Jablonowski, M. Taylor, & R. Nair (Eds.), *Numerical Techniques for Global Atmospheric Models* (pp. 381–493). Springer. https://doi.org/10.1007/978-3-642-11640-7_13

Ji, D., Fang, S., Curry, C. L., Kashimura, H., Watanabe, S., Cole, J. N. S., Lenton, A., Muri, H., Kravitz, B., & Moore, J. C. (2018). Extreme temperature and precipitation response to solar dimming and stratospheric aerosol geoengineering. *Atmospheric Chemistry and Physics*, *18*(14), 10133–10156. https://doi.org/10.5194/acp-18-10133-2018

Keith, D., Weisenstein, D., Dykema, J., & Keutsch, F. (2016). Stratospheric Solar Geoengineering without Ozone Loss. *Proceedings of the National Academy of Sciences*. http://www.pnas.org/content/113/52/14910.full

Kravitz, B., Robock, A., Boucher, O., Schmidt, H., Taylor, K. E., Stenchikov, G., & Schulz, M. (2011). The Geoengineering Model Intercomparison Project (GeoMIP). *Atmospheric Science Letters*, *12*(2), 162–167. https://doi.org/10.1002/asl.316

Legras, B., Pisso, I., Berthet, G., & Lefèvre, F. (2005). Variability of the Lagrangian turbulent diffusion in the lower stratosphere. *Atmospheric Chemistry and Physics*, *5*(6), 1605–1622. https://doi.org/10.5194/acp-5-1605-2005

Määttänen, A., Merikanto, J., Henschel, H., Duplissy, J., Makkonen, R., Ortega, I. K., & Vehkamäki, H. (2018). New Parameterizations for Neutral and Ion-Induced Sulfuric

Acid-Water Particle Formation in Nucleation and Kinetic Regimes. *Journal of Geophysical Research: Atmospheres*, *123*(2), 1269–1296. https://doi.org/10.1002/2017JD027429

Maruca, B. A., Marino, R., Sundkvist, D., Godbole, N. H., Constantin, S., Carbone, V., & Zimmerman, H. (2017). Overview of and first observations from the TILDAE High-Altitude Balloon Mission. *Atmospheric Measurement Techniques*, *10*(4), 1595–1607. https://doi.org/10.5194/amt-10-1595-2017

McCormick, M. P., Thomason, L. W., & Trepte, C. R. (1995). Atmospheric effects of the Mt Pinatubo eruption. *Nature*, *373*(6513), 399–404. https://doi.org/10.1038/373399a0

Molina, M. J., Molina, L. T., Zhang, R., Meads, R. F., & Spencer, D. D. (1997). The reaction of ClONO2 with HCl on aluminum oxide. *Geophysical Research Letters*, *24*(13), 1619–1622. https://doi.org/10.1029/97GL01560

Murphy, D. M., Telg, H., Eck, T. F., Rodriguez, J., Stalin, S. E., & Bates, T. S. (2016). A miniature scanning sun photometer for vertical profiles and mobile platforms. *Aerosol Science and Technology*, *50*(1), 11–16. https://doi.org/10.1080/02786826.2015.1121200

Nakamura, N. (1996). Two-Dimensional Mixing, Edge Formation, and Permeability Diagnosed in an Area Coordinate. *Journal of the Atmospheric Sciences*, *53*(11), 1524–1537. https://doi.org/10.1175/1520-0469(1996)053<1524:TDMEFA>2.0.CO;2

National Academy of Sciences, National Academy of Engineering, & Institute of Medicine. (1992). *Policy Implications of Greenhouse Warming: Mitigation, Adaptation, and the Science Base*. The National Academies Press. https://doi.org/10.17226/1605

National Research Council. (2015). *Climate Intervention: Reflecting Sunlight to Cool Earth*. The National Academies Press. https://doi.org/10.17226/18988

Niemeier, U., & Timmreck, C. (2015). What is the limit of climate engineering by stratospheric injection of SO2? *Atmospheric Chemistry and Physics; Katlenburg-Lindau*, *15*(16), 9129. http://dx.doi.org.ezp-prod1.hul.harvard.edu/10.5194/acp-15-9129-2015

Orsolini, Y., Simon, P., & Cariolle, D. (1995). Filamentation and layering of an idealized tracer by observed winds in the lower stratosphere. *Geophysical Research Letters*, *22*(7), 839–842. https://doi.org/10.1029/95GL00389

Phoenix, D. B., Homeyer, C. R., & Barth, M. C. (2017). Sensitivity of simulated convection-driven stratosphere-troposphere exchange in WRF-Chem to the choice of physical and chemical parameterization. *Earth and Space Science*, *4*(8), 454–471. https://doi.org/10.1002/2017EA000287

Pierce, J., Weisenstein, D., Heckendorn, P., Peter, T., & Keith, D. (2010). Efficient formation of stratospheric aerosol for climate engineering by emission of condensible vapor from aircraft. *Geophysical Research Letters*, *37*. https://doi.org/10.1029/2010GL043975

Pope, F. D., Braesicke, P., Grainger, R. G., Kalberer, M., Watson, I. M., Davidson, P. J., & Cox, R. A. (2012). Stratospheric aerosol particles and solar-radiation management. *Nature*

Climate Change, *2*(10), 713–719. https://doi.org/10.1038/nclimate1528

Prather, M., & Jaffe, A. H. (1990). Global impact of the Antarctic ozone hole: Chemical propagation. *Journal of Geophysical Research: Atmospheres*, *95*(D4), 3473–3492. https://doi.org/10.1029/JD095iD04p03473

Rauthe, M., Gerding, M., & Lübken, F.-J. (2008). Seasonal changes in gravity wave activity measured by lidars at mid-latitudes. *Atmospheric Chemistry and Physics*, *8*(22), 6775–6787. https://doi.org/10.5194/acp-8-6775-2008

Richter, J., H., Tilmes, S., Glanville, A., Kravitz, B., MacMartin, D. G., Mills, M. J., Simpson, I. R., Vitt, F., Tribbia, J. J., & Lamarque, J.-F. (2018). Stratospheric Response in the First Geoengineering Simulation Meeting Multiple Surface Climate Objectives. *Journal of Geophysical Research: Atmospheres*, *123*(11), 5762–5782. https://doi.org/10.1029/2018JD028285

Robock, A. (2000). Volcanic eruptions and climate. *Reviews of Geophysics*, *38*(2), 191–219. https://doi.org/10.1029/1998RG000054

Ross, M. N., Ballenthin, J. O., Gosselin, R. B., Meads, R. F., Zittel, P. F., Benbrook, J. R., & Sheldon, W. R. (1997). In-situ measurement of Cl2 and O3 in a stratospheric solid rocket motor exhaust plume. *Geophysical Research Letters*, *24*(14), 1755–1758. https://doi.org/10.1029/97GL01592

Ross, M. N., Whitefield, P. D., Hagen, D. E., & Hopkins, A. R. (1999). In situ measurement of the aerosol size distribution in stratospheric solid rocket motor exhaust plumes. *Geophysical Research Letters*, *26*(7), 819–822. https://doi.org/10.1029/1999GL900085

Russell, L. M., Rasch, P. J., Mace, G. M., Jackson, R. B., Shepherd, J., Liss, P., Leinen, M., Schimel, D., Vaughan, N. E., Janetos, A. C., Boyd, P. W., Norby, R. J., Caldeira, K., Merikanto, J., Artaxo, P., Melillo, J., & Morgan, M. G. (2012). Ecosystem Impacts of Geoengineering: A Review for Developing a Science Plan. *AMBIO*, *41*(4), 350–369. https://doi.org/10.1007/s13280-012-0258-5

Schneider, A., Gerding, M., & Lübken, F.-J. (2015). Comparing turbulent parameters obtained from LITOS and radiosonde measurements. *Atmospheric Chemistry and Physics*, *15*(4), 2159–2166. https://doi.org/10.5194/acp-15-2159-2015

Schneider, Andreas, Wagner, J., Söder, J., Gerding, M., & Lübken, F.-J. (2017). Case study of wave breaking with high-resolution turbulence measurements with LITOS and WRF simulations. *Atmospheric Chemistry and Physics; Katlenburg-Lindau*, *17*(12), 7941–7954. https://doi.org/10.5194/acp-17-7941-2017

Schoeberl, M. R., & Bacmeister, J. T. (1993). Mixing Processes in the Extra Tropical Stratosphere. In M.-L. Chanin (Ed.), *The Role of the Stratosphere in Global Change* (pp. 135–152). Springer. https://doi.org/10.1007/978-3-642-78306-7_5

Simpson, I. R., Tilmes, S., Richter, J. H., Kravitz, B., MacMartin, D. G., Mills, M. J., Fasullo, J. T., & Pendergrass, A. G. (2019). The Regional Hydroclimate Response to Stratospheric Sulfate Geoengineering and the Role of Stratospheric Heating. *Journal of Geophysical Research: Atmospheres*, *124*(23), 12587–12616.

https://doi.org/10.1029/2019JD031093
Söder, J., Gerding, M., Schneider, A., Dörnbrack, A., Wilms, H., Wagner, J., & Lübken, F.-J. (2019). Evaluation of wake influence on high-resolution balloon-sonde measurements. *Atmospheric Measurement Techniques*, *12*(8), 4191–4210. https://doi.org/10.5194/amt-12-4191-2019
Sparling, L. C., & Bacmeister, J. T. (2001). Scale dependence of tracer microstructure: PDFs, intermittency and the dissipation scale. *Geophysical Research Letters*, *28*(14), 2823–2826. https://doi.org/10.1029/2000GL012781
Stolarski, R. S., & Wesoky, H. L. (1993). *The atmospheric effects of stratospheric aircraft*. NASA. http://ntrs.nasa.gov/search.jsp?R=19930013868
Sukhodolov, T., Sheng, J.-X., Feinberg, A., Luo, B.-P., Peter, T., Revell, L., Stenke, A., Weisenstein, D. K., & Rozanov, E. (2018). Stratospheric aerosol evolution after Pinatubo simulated with a coupled size-resolved aerosol–chemistry–climate model, SOCOL-AERv1.0. *Geoscientific Model Development*, *11*(7), 2633–2647. https://doi.org/10.5194/gmd-11-2633-2018
Teller, E., Wood, L., & Hyde, R. (1996). *Global warming and ice ages: I. prospects for physics based modulation of global change* (UCRL-JC-128715; CONF-9708117-). Lawrence Livermore National Lab., CA (United States). https://www.osti.gov/biblio/611779-global-warming-ice-ages-prospects-physics-based-modulation-global-change
Theuerkauf, A., Gerding, M., & Lübken, F.-J. (2011). LITOS – a new balloon-borne instrument for fine-scale turbulence soundings in the stratosphere. *Atmospheric Measurement Techniques*, *4*(1), 55–66. https://doi.org/10.5194/amt-4-55-2011
Tilmes, S., Fasullo, J., Lamarque, J.-F., Marsh, D. R., Mills, M., Alterskjær, K., Muri, H., Kristjánsson, J. E., Boucher, O., Schulz, M., Cole, J. N. S., Curry, C. L., Jones, A., Haywood, J., Irvine, P. J., Ji, D., Moore, J. C., Karam, D. B., Kravitz, B., … Watanabe, S. (2013). The hydrological impact of geoengineering in the Geoengineering Model Intercomparison Project (GeoMIP). *Journal of Geophysical Research: Atmospheres*, *118*(19), 11,036-11,058. https://doi.org/10.1002/jgrd.50868
Tilmes, S., Richter, J. H., Kravitz, B., MacMartin, D. G., Mills, M. J., Simpson, I. R., Glanville, A. S., Fasullo, J. T., Phillips, A. S., Lamarque, J.-F., Tribbia, J., Edwards, J., Mickelson, S., & Ghosh, S. (2018). CESM1(WACCM) Stratospheric Aerosol Geoengineering Large Ensemble Project. *Bulletin of the American Meteorological Society*, *99*(11), 2361–2371. https://doi.org/10.1175/BAMS-D-17-0267.1
Torres, B., Dubovik, O., Toledano, C., Berjon, A., Cachorro, V. E., Lapyonok, T., Litvinov, P., & Goloub, P. (2014). Sensitivity of aerosol retrieval to geometrical configuration of ground-based sun/sky radiometer observations. *Atmospheric Chemistry and Physics*, *14*(2), 847–875. https://doi.org/10.5194/acp-14-847-2014
Vanneste, J. (2004). Small-Scale Mixing, Large-Scale Advection, and Stratospheric Tracer Distributions. *Journal of the Atmospheric Sciences; Boston*, *61*(22), 2749–2761.
Vattioni, S., Weisenstein, D., Keith, D., Feinberg, A., Peter, T., & Stenke, A. (2019). Exploring accumulation-mode H2SO4 versus SO2 stratospheric sulfate geoengineering in a

sectional aerosol–chemistry–climate model. *Atmospheric Chemistry and Physics*, *19*.

Vehkamäki, H., Kulmala, M., Napari, I., Lehtinen, K. E. J., Timmreck, C., Noppel, M., & Laaksonen, A. (2002). An improved parameterization for sulfuric acid–water nucleation rates for tropospheric and stratospheric conditions. *Journal of Geophysical Research: Atmospheres*, *107*(D22), AAC 3-1-AAC 3-10. https://doi.org/10.1029/2002JD002184

Voigt, C., Schumann, U., Graf, K., & Gottschaldt, K.-D. (2013). Impact of rocket exhaust plumes on atmospheric composition and climate — an overview. *Progress in Propulsion Physics*, *4*, 657–670. https://doi.org/10.1051/eucass/201304657

Weisenstein, D., Keith, D., & Dykema, J. (2015). Solar geoengineering using solid aerosol in the stratosphere. *Atmospheric Chemistry and Physics*, *15*, 11835–11859. https://doi.org/10.5194/acp-15-11835-2015

World Meteorological Organization, United States, National Oceanic and Atmospheric Administration, United States, National Aeronautics and Space Administration, United Nations Environment Programme, & European Commission. (2019). *Scientific assessment of ozone depletion: 2018.*

Yu, F., & Turco, R. P. (1997). The role of ions in the formation and evolution of particles in aircraft plumes. *Geophysical Research Letters*, *24*(15), 1927–1930. https://doi.org/10.1029/97GL01822

Supplemental Materials

Dai, Z., F. Keutsch, D. Weisenstein, and D. W. Keith. (2020). Experimental reaction rates constrain estimates of ozone response to calcium carbonate geoengineering, *Manuscript submitted for publication.*

Dykema, J., Keith, D., Anderson, J. G., & Weisenstein, D. (2014). Stratospheric controlled perturbation experiment (SCoPEx): A small-scale experiment to improve understanding of the risks of solar geoengineering. *Philosophical Transactions of the Royal Society A*, *372*. https://doi.org/10.1098/rsta.2014.0059

Dykema, J., Keith, D., & Keutsch, F. (2016). Improved aerosol radiative properties as a foundation for solar geoengineering risk assessment. *Geophysical Research Letters*. http://onlinelibrary.wiley.com/doi/10.1002/2016GL069258/full

Floerchinger, C., J. Dykema, D. Keith, F. Keutsch. (2020). A Need For In Situ Observations to Inform Nearfield Plume Transport and Aerosol Dynamics as well as Chemistry of Alternate Geoengineering Materials in the Stratosphere. *Letter to the National Academy for Science.*

Golja, C. M., L. W. Chew, J. A. Dykema, and D. W. Keith. (2020). Aerosol Dynamics in the Near Field of the SCoPEx Stratospheric Balloon Experiment, *Manuscript submitted for publication.*

Keith, D., F. Keutsch, C. Floerchinger. (2020). Empirical methods to reduce uncertainty about solar geoengineering. *Submitted as public input to the National Academy Committee on Climate Intervention Strategies that Reflect Sunlight to Cool Earth.*